Agricultural Water Management 271 (2022) 107734

Contents lists available at ScienceDirect

Agricultural Water Management

journal homepage: www.elsevier.com/locate/agwat

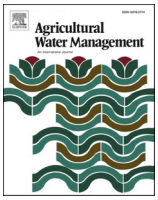

Towards an operational irrigation management system for Sweden with a water–food–energy nexus perspective

P.E. Campana [a,*], P. Lastanao [a], S. Zainali [a], J. Zhang [b], T. Landelius [c], F. Melton [d,e]

[a] Mälardalen University, Department of Sustainable Energy Systems, Västerås, SE 72123, Sweden
[b] Uppsala University, Department of Earth Sciences, Uppsala, SE 75236, Sweden
[c] Swedish Meteorological and Hydrological Institute, Norrköping, SE 60176, Sweden
[d] NASA Ames Research Center Cooperative for Research in Earth Science and Technology (NASA ARC-CREST), Moffett Field, CA 94035, USA
[e] California State University, Monterey Bay, Seaside, CA 93955, USA

ARTICLE INFO

Keywords:
Water–food–energy nexus
Drought
Irrigation
Data visualization

ABSTRACT

The 2018 drought in Sweden prompted questions about climate-adaptation and -mitigation measures – especially in the agricultural sector, which suffered the most. This study applies a water–food–energy nexus modelling framework to evaluate drought impacts on irrigation and agriculture in Sweden using 2018 and 2019 as case studies. A previous water–food–energy nexus model was updated to facilitate an investigation of the benefits of data-driven irrigation scheduling as compared to existing irrigation guidelines. Moreover, the benefits of assimilating earth observation data in the crop model have been explored. The assimilation of leaf area index data from the Copernicus Global Land Service improves the crop yield estimation as compared to default crop model parameters. The results show that the irrigation water productivities of the proposed model are measurably improved compared to conventional and static irrigation guidelines for both 2018 and 2019. This is mostly due to the advantage of the proposed model in providing evapotranspiration in cultural condition (ET_c)-driven guidelines by using spatially explicit data generated by mesoscale models from the Swedish Meteorological and Hydrological Institute. During the drought year 2018, the developed model showed no irrigation water savings as compared to irrigation scenarios based on conventional irrigation guidelines. Nevertheless, the crop yield increase from the proposed irrigation management system varied between 10% and 60% as compared to conventional irrigation scenarios. During a normal year, the proposed irrigation management system leads to significant water savings as compared to conventional irrigation guidelines. The modelling results show that temperature stress during the 2018 drought also played a key role in reducing crop yields, with yield reductions of up to 30%. From a water–food–energy nexus, this motivates the implementation of new technologies to reduce water and temperature stress to mitigate likely negative effects of climate change and extremes. By using an open-source package for Google Earth®, a demonstrator of cost-effective visualization platform is developed for helping farmers, and water- and energy-management agencies to better understand the connections between water and energy use, and food production. This can be significant, especially during the occurrence of extreme events, but also to adapt to the negative effects on agricultural production of climate changes.

1. Introduction

In 2018, Sweden experienced an unprecedented drought that severely affected the agricultural, water, and energy sectors. During the period from June to July 2018, some regions experienced a significant reduction in precipitation as compared to a normal year. Krikken et al. (2019) showed a precipitation anomaly for July 2018 ranging from 0 mm to −100 mm as compared to 1981–2010 climatology. In July 2018, some locations, such as Kastlösa in Öland and Komstorp in Blekinge, did not receive any precipitation, while others, such as Varberg and Öland's southern cape, received 0.2 and 0.8 mm, respectively (SMHI, 2020a). This caused a drastic reduction in crop yields, including for key crops such as wheat, potatoes, and other forage crops. The lack of forage crops negatively affected dairy farms and related industry. Analysis of the Standardized Precipitation-Evapotranspiration Index (SPEI) for the period 1950–2020 indicates that 2018 was one of the worst droughts in

* Corresponding author.
E-mail address: pietro.campana@mdu.se (P.E. Campana).

https://doi.org/10.1016/j.agwat.2022.107734
Received 12 April 2021; Received in revised form 15 April 2022; Accepted 16 May 2022
Available online 15 June 2022

more than 50 years for Swedish farmers (SPEI Global Drought Monitor, 2020). As a result, farmers had to start irrigating or installing irrigation systems. However, the scarcity of rainfall also severely affected the water resources available for agricultural production. Some counties, such as Skåne, issued restrictions on irrigation to preserve the scarce water resources, putting further stress on farmers, especially those who had water-intensive crops, such as vegetables and potatoes (The Local, 2020). In some cases, especially for those growers who did not have the possibility of irrigation, potatoes were unharvested due to the poor yield and potatoes size (Statistics Sweden, 2022a). Compared to southern European countries, such as Greece, Italy or Spain, where irrigation is a more well-established practice, Swedish farmers have generally lacked adequate means and incentives to determine water-use requirements for crops, to schedule irrigation applications to match crop water requirements, to evaluate the response of crop yields to different water management practices, and to evaluate current on-farm water-efficiency levels. The combination of these factors led to the worst crop harvest since the 1950s for Sweden (Bioenergy International, 2020). The extreme drought also affected the energy sector. Higher volumes of water pumped for irrigation required higher electricity demand in the agricultural sector. Low precipitation levels affected hydropower generation due to low refilling volumes. The state-owned power company Vattenfall AB closed the 900-MW number 2 nuclear reactor at its Ringhals power plant since the water required for the cooling process reached high temperatures that could threaten the safety and function of the reactor (Renew Economy, 2020). This acute drought event in Sweden clearly highlighted the water–food–energy (WFE) nexus interrelationships and how they can be exacerbated during extreme events. Moreover, the climate-change scenarios produced by the Swedish Meteorological and Hydrological Institute (SMHI) predict that the annual mean temperature in Sweden will grow steadily from now until the year 2100 and beyond (Belusic et al., 2019). The precipitation patterns from climate models show high variability, indicating that drought events and heat waves will likely happen more frequently, with socio-economic consequences in several sectors. As highlighted by Belusic et al. (2019), studies on drought and drought effects on water balance calculations in Scandinavia are limited. Sweden needs to account for increasing drought frequency and severity as part of ongoing planning efforts to mitigate the potential effects of climate change and extreme weather phenomena. In 2018, the Swedish Government presented a national crisis package valued at more than SEK 1.2 billion (SEK 1 ≈ USD 0.1), primarily to cover the fodder shortage and other losses of income that farmers experienced due to the drought. SEK 760 million were invested in 2019 to develop measures to alleviate the situation for the drought-affected agricultural sector (Government Offices of Sweden, 2020). Recently, Grusson et al. (2021a) analyzed the impacts of climate change on the Swedish agriculture, highlighting the increasing need for irrigation, especially during the beginning of the growing season due to the higher probability of dry springs. Grusson et al. (2021b) also highlighted that future climate change scenarios predict an increase in precipitation in Sweden. Nevertheless, the predicted increase in precipitation, especially in the South of Sweden, will not lead to increased soil moisture for supporting crop production, but to an increased run-off since the precipitations events will increase in intensity. The SMHI provides a water-shortage risk service through an overview of groundwater levels, surface water levels, and statistical summaries of precipitation amounts. However, this service does not incorporate any dynamic satellite information regarding soil moisture and vegetation characteristics. Currently, only general irrigation guidelines, based on the Penman–Monteith equation (Allen et al., 1998) are provided. In addition, existing guidelines sometimes suggest different values. For instance, Bergström and Barkefors (2004) suggested irrigating potatoes with 100 mm/season on average (maximum 200 mm/season). The Swedish Board of Agriculture (2007) mentioned that water requirements for potatoes should be between 300 and 350 mm, assuming average precipitation of between 170 and 250 mm during the same period. The report from the Swedish Board of Agriculture (2007) also provided static guidelines for the irrigation of potatoes for different locations, e.g., Visby (57.6348° N, 18.2948° E) with 130 mm/season recommended, and Umeå (63.8258° N, 20.2630° E) with 75 mm/season recommended. No irrigation management services are provided in Sweden, unlike in countries or regions that historically have been more prone to drought. In addition, the input data for irrigation and for nutrient management depend on spatio-temporal data such as climatological and soil-type data, and this heterogeneity requires spatially explicit information to produce accurate guidelines. For this reason, researchers and institutions have been active in developing decision-support systems based on simulation and optimization models, or satellite data observations, or hybrid approaches, to provide guidelines on optimal irrigation and nutrient applications and thus to inform smart farming management.

The NASA Satellite Irrigation Management Support (SIMS) system (Melton et al., 2012; Pereira et al., 2020, 2021) integrates Earth observation data from Landsat and MODIS with meteorological observations to generate daily maps of evapotranspiration (*ET*) and eight-day maps of crop coefficients over California. The newly launched OpenET (2021) has implemented six satellite-based *ET* models on the Google Earth Engine platform (Gorelick et al., 2017) to develop daily, monthly, and annual *ET* database for the western US easily available at field scales (30 m × 30 m per pixel) via a web-based UI and application programming interface (API). The OpenET models intercomparison and accuracy assessment has been carried out through different phases by relying on 70 (first phase) and 69 (second phase) data from flux towers across the United States of America (Melton et al., 2021). Wang et al. (2019) developed a web-based irrigation decision support system for canal irrigation management. The model is based upon two modules. The first module is for real-time irrigation forecasting and scheduling. The second module is for planning the canals' water delivery volumes. In Italy, IRRINET is a decision-support system for on-farm irrigation scheduling (Mannini et al., 2013) that gives farmers day-by-day information on how much and when to irrigate crops. The system implements a real-time irrigation scheduling through climatic and meteorological data gathered daily. Another example of decision support system in Italy is FERTIRRIGERE (Battilani, 2004), a model-based decision-support system used in Italy that proved to reduce the nitrogen application on horticultural products by 46% compared to conventional practices, with no notable effects on yield and quality. Mahmoud and Gan (2019) developed a model to enhance the irrigation water management in central Saudi Arabia by assessing the spatio-temporal variation of actual evapotranspiration through remote sensing techniques and meteorological data. Zhang et al. (2012) developed the ZhaoKou irrigation management system, consisting of a precipitation forecasting module, a crop water demand forecasting module, and a crop coefficient index. The established system improved water efficiency, providing a theoretical basis for water resources scheduling and channels' rational control. Galindo et al. (2017) presented a methodology for optimal water and energy management in the irrigation system using a two-layer management scheme. The upper layer is an optimal control strategy to plan how to serve the required water within a five-day prediction horizon to minimize pumping electricity costs. The lower layer is a scheduling algorithm that decides how to schedule the different pumps to supply the desired flow, minimize cost, and maximize efficiency. In Romania, a field-scale irrigation planning and management system was set up and tested (FutureWater, 2020). Irrigation guidelines are provided by integrating soil moisture content ground data with hydrological model calculations. In Greece, agriculture – and especially irrigation – plays a key role in terms of water management, and the IRMA_SYSTEM (2021) calculates site-specific crop water requirements and irrigation scheduling at high spatial resolution (Malamos et al., 2015). The decision-support system integrates historical and forecast agrometeorological data, crop data, and soil data to provide timely guidelines for irrigation. A comprehensive review of irrigation and

fertilization decision support systems is provided in Gallardo et al. (2020).

The WFE nexus concept was introduced during the 2008 World Economic Forum to discuss the important interlinkages among the water, food, and energy sectors highlighted by the global food security crisis of 2008 (Dominic, 2011). The agricultural and food production sectors are at the center of the nexus concept because both sectors require significant amounts of water and energy for irrigation and food production: 70% of the global water withdrawals and 30% of the world's total energy consumption are allocated to this sector (Food and Agriculture Organization (FAO), 2017). Since research on the nexus began, several modelling tools have been developed. Nevertheless, most of the modelling approaches have only looked at interactions between two out of the three sectors, which is not optimal for improving the efficiency of resources (Kaddoura and El Khatib, 2017). Moreover, very few models are at the stage of implementing the WFE nexus approach (Liu et al., 2017; Dai et al., 2018; Shannak et al., 2018; Endo et al., 2019) or supporting political decisions (Bazilian et al., 2011). Furthermore, as highlighted by Lawford (2019), there is a general data gap, in both spatial and temporal dimensions, concerning the observation of key parameters for WFE nexus analysis. Most of the current available irrigation management systems lack a WFE perspective that integrates information concerning irrigation water requirements, crop response to irrigation, and energy consumption. This study aims to lay the foundations to develop an operational WFE nexus irrigation management system for Sweden, by including all three areas of the nexus. This is attained by using the spatially explicit climatic data generated by SMHI. Specific objectives of this study are to:

- further develop the model presented in Zhang et al. (2018) for Nebraska and in Campana et al. (2018) for Sweden by implementing the Penman–Monteith equation for the calculation of reference evapotranspiration, and related improvement and validation using remote-sensing data and tower flux data;
- analyze the irrigation water productivity of existing irrigation guidelines in Sweden and compare the results with the guidelines provided by the developed model;
- analyze WFE nexus aspects related to irrigation systems in Sweden;
- develop a demonstrator for a future operational service, primarily for farmers interested in crop conditions and irrigation guidelines, but also for energy- and water-management-related agencies.

To our best knowledge, there is no irrigation management system in Sweden as compared to other countries in Asia, or Europe, or United States of America. Moreover, although the 2018 drought has triggered research activities on irrigation, from our literature review few studies have been carried out in Sweden on irrigation and especially for combating and adapting to climate changes. This was also clearly highlighted in Grusson et al. (2021a). The novelty of this study lies mainly in three points:

- develop a demonstrator of irrigation management system, called SWEDish Irrigation Management System (SWEDIMS, 2022), combined with the gridded meteorological products developed by SMHI for retrieving climatological data;
- develop a model-based management system that can be used to provide information not only for evapotranspiration, but also to crop grow when combined with a crop model and with earth observations;
- develop a model not only for providing irrigation management guidelines but also extending the model functionalities to work as a WFE nexus model within the irrigation-agricultural sector in Sweden.

Although the model presented in this study is applied to Sweden using gridded data generated by two mesoscale models (STRÅNG, 2020) and MESAN (SMHI, 2020b) from the SMHI, it has general validity and can be extended to other regions using different gridded products for climatological variables.

The paper is organized as follows: the problem statement and the objective of this study are introduced in Section 1, which also provides a literature review of irrigation management systems. Data and methods are presented in Section 2. The main results of this study (i.e., model validation, irrigation water productivity for three irrigation guidelines scenarios, water–food energy nexus relationships in the irrigation sector, and visualization) are presented in Section 3. The conclusions of this study are summarized in Section 4.

2. Data and methods

2.1. Data

The gridded meteorological data used to generate the results are mainly taken from the mesoscale models STRÅNG (2020) and MESAN (SMHI, 2020b) that are developed by SMHI. In the study carried out by Grusson, Barron (2021c), MESAN, which covers a large part of northern Europe, provided a better representation of the agro-climatological variables used to depict dry and wet days and spells as compared to other gridded products. We have used 2018 as a case study, due to the serious drought that affected the entire country that year, and 2019 as a normal year. The crop model used in this study refers to the model developed by Williams et al. (1989). A more detailed description of the WFE nexus model can be found in Zhang et al. (2018) and Campana et al. (2018). The crop mask was built upon data provided by the Swedish Board of Agriculture (2020). The groundwater depth dataset refers to the product developed by Fan et al. (2013). The soil field capacity and wilting point are from the Global Soil Data Task Group (2000). The irrigation areas refer to Food and Agriculture Organization (2016). The leaf area index (*LAI*) used for improving the *LAI* sub model is from Copernicus Global Land Service (2020). The 2018 flux tower data were retrieved from the Integrated Carbon Observation System (ICOS) Sweden (ICOS, 2019). Only one flux tower located at the agricultural research station of Lanna (58°20′ N, 13°06′ E, 75 m a.s.l.) was used for validation, since it was the only available flux tower installed on an agricultural field in Sweden. The data refers to one single year and crop. A detailed description of the station and related measured variables can be found in ICOS (2021). Agricultural statistics were provided through personal communication with the station principal investigator (Weslien, 2020).

2.2. Model updates and validation

As compared to the model presented in Campana et al. (2018), where the daily reference evapotranspiration (ET_o) (mm/day) was calculated using the Hargreaves and Samani equation (Hargreaves and Samani, 1982), in this study, ET_o has been calculated using the FAO-56 Penman–Monteith equation (Allen et al., 1998):

$$ET_o = \frac{0.408\Delta(R_n - G) + \gamma \frac{900}{T+273} u_2 (e_s - e_a)}{\Delta + \gamma(1 + 0.34u_2)}, \quad (1)$$

where, Δ is the saturation slope of the vapor pressure curve at T_a (kPa/°C), R_n is the net radiation (MJ/m^2/day), G is the soil heat flux density (MJ/m^2/day), γ is the psychrometric constant (kPa/°C), T is the daily mean air temperature (°C), e_s is saturation vapor pressure (kPa), e_a is the average daily actual vapor pressure (kPa), and u_2 is the daily average wind speed (m/s). Zotarelli et al. (2010) have presented a detailed guideline for the step-by-step calculation of ET_o.

In this study, the actual ET (ET_a) estimates, generated using the model and meteorological datasets described in Section 2.1, have been validated using the data measured from the flux tower installed at the ICOS agricultural research station of Lanna (ICOS, 2019). The measurements refer to latent heat flux and soil water content in 2018. The

flux tower's ET_a is calculated with the following equation from Gu et al. (2017):

$$ET_a = \frac{LEs}{\lambda \rho_a}, \quad (2)$$

where, LE is the latent heat flux (W/m^2), s is the time (s), λ is the latent heat of vaporization (J/kg), and ρ_a is the air density (kg/m^3). λ is calculated as follows (Moorhead et al., 2019):

$$\lambda = (2.501 - 0.0236T_s)10^6, \quad (3)$$

where, T_s is the surface temperature (°C). The surface temperature has been assumed to be equal to air temperature, as in Jungqvist et al. (2014). In SWEDIMS, ET_a is calculated using a water balance approach (Allen et al., 1998). To calculate the water balance, we considered that in 2018 oat was grown at the ICOS agricultural research station of Lanna (Weslien, 2020). The crop model was thus set up for oats to calculate both water-balance and crop-yield. The ET in cultural conditions (ET_c), a key component in the water balance, was calculated with an iterative approach that minimizes the root mean square error (RMSE) between the ET_c curve based on the FAO guidelines for oat development stages and corresponding cultural factors (Allen et al., 1998), and the ET_c curve described by the following equation (DeJonge et al., 2012):

$$ET_c = ET_o\left(a + b\left(1 - e^{-cLAI}\right)\right). \quad (4)$$

Eq. 4 depends on the LAI (m^2/m^2) that is computed in the model through iterations (Zhang et al., 2018). The main engine of the crop model is Eq. 5 (Williams et al., 1989):

$$Y_a = HIA \sum_{i=1}^{N} 0.001 BEPAR_{tot,i}\left(1 - e^{-0.65LAI_i}\right)\gamma_{reg,i}, \quad (5)$$

where, Y_a is the actual crop yield (t/ha), HIA is the adjusted harvest index at maturity, i is the i-th day from planting to harvesting, N is the number of days from planting to harvesting, BE is the biomass–energy ratio ((kg/ha)/(MJ/m^2)), $PAR_{tot,i}$ is the total intercepted daily Photosynthetically Active Radiation (PAR) (MJ/m^2), LAI_i is the daily leaf area index (m^2/m^2), and $\gamma_{reg,i}$ is the daily crop growth regulating factor that is the lowest values among the daily water, temperature, aeration, and nutrient stresses. A summary of the key model parameters for oats is given in Table 1.

To improve the model accuracy, we assimilated remote-sensing data for LAI into the crop model. From the LAI data, significant information can also be deducted, such as the approximate crop planting date and the parameters of the leaf area development curve. Three scenarios have been considered. In the first scenario (S1-LAI), the LAI is calculated as in Zhang et al. (2018) by using the default values as in Williams et al. (1989). In the second scenario (S2-LAI), the LAI values for the closest coordinates at Lanna research station are retrieved from the Copernicus Global Land Service (CGLS, 2020) and fed directly into the model. In the last scenario (S3-LAI), the data assimilation is performed by minimizing the RMSE (i.e., the RMSE is the function $f(x)$ to be minimized with x decisional variables) between the data generated by the developed model and the data from CGLS. The approach implemented in this study is similar to the approach used by Novelli et al. (2019) and Wagner et al. (2020). The optimization model set up is as follows:

$$\min_x f(x), \quad f(x) = RMSE = \sqrt{\frac{1}{n}\sum_{i=1}^{n}\left(LAI_{sim,i} - LAI_{CGLS,i}\right)^2}, \quad (6)$$

where, n is the number of observations, $LAI_{sim,i}$ is the simulated LAI for the day of the year corresponding to the i-th satellite derived observation from CGLS, and $LAI_{CGLS,i}$ is the LAI value from CGLS. The optimization is performed through a genetic algorithm (GA), one of the most popular meta-heuristic optimization methods mimicking biological evolution (Konak et al., 2006) and using as algorithm a variant of Non-dominated Sorting Genetic Algorithm II (NSGA-II) (Deb et al., 2000). GA is available in the Matlab® Global Optimization Toolbox. The main configuration parameters (i.e., population size, maximum number of generations, crossover fraction, and function tolerance) were set based on Matlab® Global Optimization Toolbox suggestions. The decisional variables x of the optimization were the key parameters that define the LAI curve: the planting date, the growing season, the points that define optimal LAI development curve, the LAI decline factor, and the fraction of the growing season at which the LAI starts to decline. The implementation of more advanced data assimilation algorithms (Jin et al., 2018), such as Kalman Filter (KF) or Ensemble Kalman Filter ($EnKF$), is not included in this work because that is beyond its scope. Since this study has mainly focused on the comparison between irrigation guidelines, as described in more detail in Section 2.3, the data assimilation is not applied in the calculation of the irrigation productivity while performing gridded simulations.

Table 1
Crop model parameters for oats.

Parameter	Value	Reference
Harvest index	0.42	(Williams et al., 1989)
Biomass energy ratio ((kg/ha)/(MJ/m^2))	35	(Williams et al., 1989)
Base temperature (°C)	0	(Williams et al., 1989)
Optimal temperature (°C)	15	(Williams et al., 1989)
Maximum LAI (m^2/m^2)	4	(Myrbeck, 1998)
Water stress–yield factor	0.21	(Williams et al., 1989)
Potential heat units (°C)	1450	(Balkovič et al., 2013)
LAI declining factor	1	(Williams et al., 1989)
Fraction of growing season when leaf area declines	0.8	(Williams et al., 1989)
First point on optimal leaf area development curve (%)	15.01	(Williams et al., 1989)
Second point on optimal leaf area development curve (%)	50.95	(Williams et al., 1989)

2.3. Irrigation management scenarios

Although there is motivation to improve farm irrigation management to increase production, profit, and water-use efficiency, it must be pointed out that currently, in Sweden, only general irrigation guidelines are provided, for instance by Bergström and Barkefors (2004), combined with local experiences or tools developed for other agro ecologies outside of Sweden. There is thus a need for tools and services to be designed for Swedish crop and climate conditions (Barron, 2020). In this study, we focused on two counties in the south of Sweden – Blekinge and Skåne; they belong to statistical region SE22, which has the highest water consumption for irrigation, as shown in Fig. 1.

Blekinge and Skåne have also the highest percentages of irrigated areas among croplands, the latter having markedly the higher of the two, as shown in Fig. 2 (Food and Agriculture Organization, 2016). We used potato as a reference crop, as in Campana et al. (2018), since it is the most irrigated crop in Sweden (Brundell et al., 2008). The total areas cultivated with potatoes in Blekinge and Skåne in 2018 were 2050 and 10,820 ha, respectively (Statistics Sweden, 2018). For model cross validation, the main crop model parameters were taken mostly from Jennings et al. (2020) and summarized in Table 2. The potato yield is accounted as 80% of the total biomass as in Zhou et al. (2016).

Johnson et al. (2016) analyzed the differences between irrigation following standard practices and irrigation based on decision support models that incorporate information on ET, such as the NASA SIMS model (Melton et al., 2012; Pereira et al., 2020, 2021). Based on two

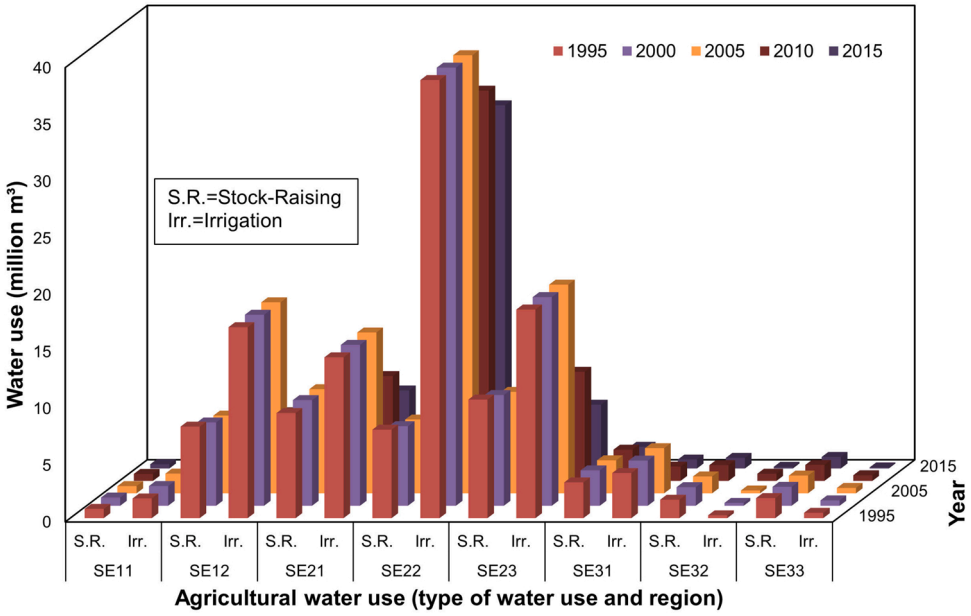

Fig. 1. Agricultural water use, by type of water use and region, 1995–2015 (Statistics Sweden, 2021).

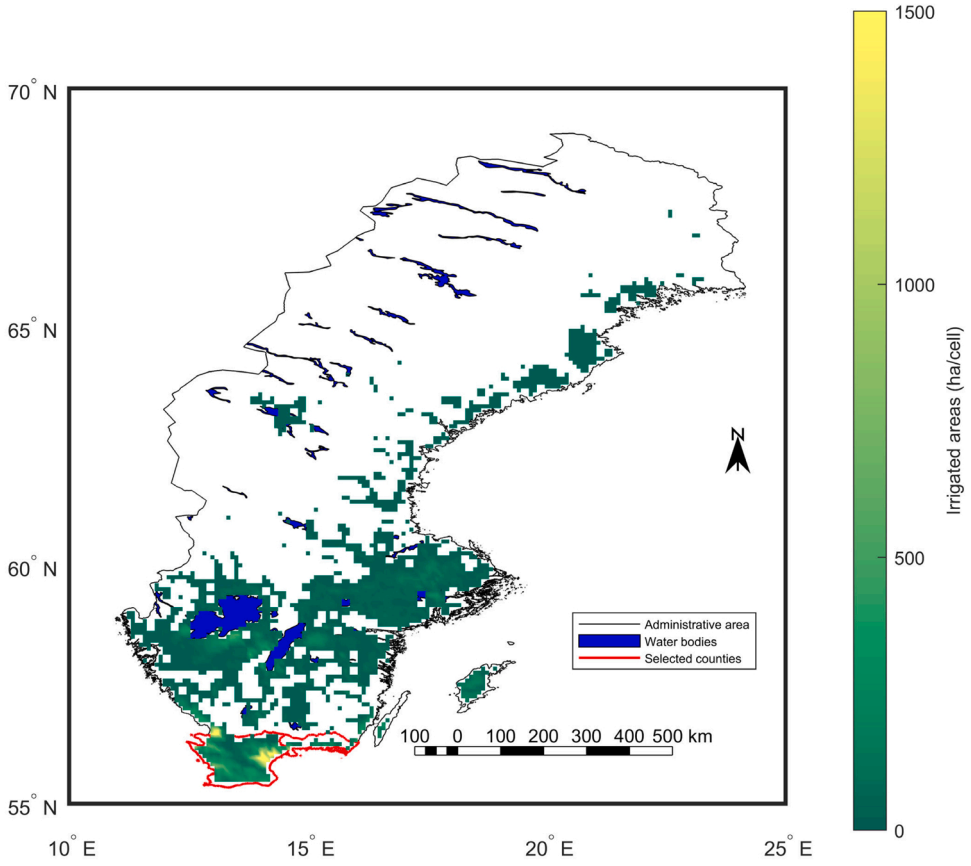

Fig. 2. Irrigated areas in Sweden (Food and Agriculture Organization, 2016).

years of field data collected for head lettuce and broccoli using a randomized block design, the authors found that standard practices led to an increase in water consumption between 26% and 40% for lettuce and between 39% and 51% for broccoli, as compared to *ET*-based irrigation management strategies based on data from SIMS. Crop yields and qualities were very similar among the treatments, and no statistically significant differences in crop yield or quality differences were observed. Inspired by the results achieved by Johnson et al. (2016), we developed three scenarios to analyze the impact of an irrigation management service as compared to conventional irrigation guidelines on the irrigation water productivity (*IWP*) (kg/m^3) and water savings. The *IWP* is defined as the ratio between the difference in crop yield with and without

Table 2
Crop model parameters for potatoes.

Parameter	Value	Reference
Harvest index	0.8	(Jennings et al., 2020)
Biomass energy ratio ((kg/ha)/(MJ/m^2))	27	(Jennings et al., 2020)
Base temperature (°C)	4	(Jennings et al., 2020)
Optimal temperature (°C)	18	(Jennings et al., 2020)
Maximum LAI (m^2/m^2)	2.8	(Jennings et al., 2020)
Water stress–yield factor	0.6	(Jennings et al., 2020)
Potential heat units (°C)	1600	(Jennings et al., 2020)
LAI declining factor	1	(Williams et al., 1989)
Fraction of growing season when leaf area declines	0.6	(Williams et al., 1989)
First point on optimal leaf area development curve (%)	15.01	(Williams et al., 1989)
Second point on optimal leaf area development curve (%)	50.95	(Williams et al., 1989)

irrigation and the water applied through irrigation as in Bos (1985) and in Stepanovic et al. (2021). Three scenarios were defined for the irrigation requirements: in the first scenario (S1-irrigation ET), the irrigation demand follows the guidelines generated by the model developed in this study. According to Bergström and Barkefors (2004), 70% of the potato area is irrigated with an average of 100 mm/season up to 200 mm/season with three to four irrigation events. Slightly different values were presented in the report from the Swedish Board of Agriculture (2007), where the seasonal water requirement for potato was between 300 and 350 mm, assuming a rainfall of 170–250 mm during the irrigation season.

Based on those two static guidelines, we have thus considered two further scenarios: S2-irrigation static 100 consists of three irrigation events for a total of 100 mm/season, while S3-irrigation static 150 consisted in applying 150 mm in four events. A summary of the scenarios is provided in Table 3. The results among irrigation guidelines are compared in terms of *IWP* (kg/m^3). The irrigation follows an operational strategy similar to that of solar irrigation systems, which provide an optimal dynamic match between water demand and supply (Campana et al., 2015; Zhang et al., 2018). As compared to the previous studies (Campana et al., 2018; Zhang et al., 2018), where we assumed constant soil moisture was to be maintained, in this study irrigation is performed only when the water stress coefficient (K_s) as defined by Allen et al. (1998) goes below 1.0. Unlike in previous studies (Campana et al., 2018; Zhang et al., 2018), no optimization is performed or investigated in this study.

Table 3
Irrigation scenarios definition.

Sensitive parameter	S1-irrigation ET	S2-irrigation static 100	S3-irrigation static150
Irrigation method	Sprinkler	Sprinkler	Sprinkler
Irrigation efficiency	90%	90%	90%
Description	Water provided according to scheduling proposed by model developed in this study based on the K_s value	3 irrigation events totaling 100 mm/season	4 irrigation events totaling 150 mm/season
Derived from	–	Bergström and Barkefors (2004), 3–4 irrigation events totaling 100–200 mm/season	Swedish Board of Agriculture (2007), total water requirement 300–350 mm assuming rainfall of 170–250 mm/season

2.4. The water–energy nexus

The energy consumption of irrigation systems depends mainly on irrigation water volumes, hydraulic head, and pumping system. Several other aspects such as irrigation strategy, irrigation system, and fuel affect those factors. Eq. 7 summarizes all these parameters to allow a comprehensive calculation of the energy requirements for irrigation E_{irr} (kWh):

$$E_{irr} = cf1\,\frac{cf2\,\frac{ET_c - P_e}{\eta_{irr}(1-LR)}A(\mathrm{SH} + \mathrm{d} + \quad \mathrm{H}_{irr} \quad + \quad \sum\lambda + \sum\zeta)}{\eta_m \eta_p}, \tag{7}$$

Where, *cf1* is a conversion factor equal to 0.0027 that takes into consideration the density of water (1000 kg/m^3), gravity acceleration (9.8 m/s^2), and the conversion between Joule and kWh (1/(3.6·10^6)), *cf2* converts mm into m, ET_c is the evapotranspiration in cultural conditions (mm), P_e is the effective precipitation (mm), A is the irrigated area (m^2), η_{irr} is the efficiency of the irrigation system (%), LR is the leaching requirement (%), SH is the static head (m), d is the drawdown (m), H_{irr} is the required head to operate the irrigation system (m), λ and ξ are continuous and concentrated head losses (m), η_m is the motor efficiency (%), and η_p is the pump efficiency (%). The drawdown depends on the specific borehole performance, and it is site-specific as it varies with the geological properties of the location (e.g., permeability, storage capacity). An overview of the parameters affecting the energy

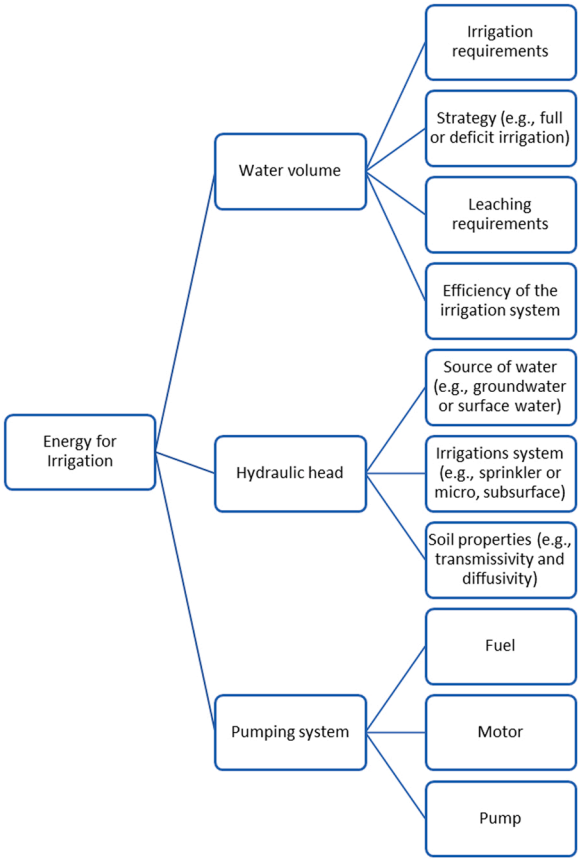

Fig. 3. Parameters affecting energy consumption in irrigation systems.

consumption of irrigation system is given in Fig. 3. From a WFE nexus perspective, Eq. 7 encapsulates the relationships among water, energy, food, and soil for irrigation systems. The soil aspect of Eq. 7 is related to the irrigation scheduling, which typically depends on field capacity and the soil wilting point. The irrigation frequency I_{freq} (1/day) is calculated as the ratio between the irrigation water requirements (mm/day) and the irrigation height (mm):

$$I_{freq} = \frac{\frac{ET_c - P_e}{\eta_{irr}(1-LR)}}{f(\theta_{fc} - \theta_{wp})d}, \quad (8)$$

where, f is the fraction of the total available water that can be used by the plant without stress, θ_{fc} is the soil field capacity (mm/m), θ_{wp} is the soil wilting point (mm/m), and d is the crop root depth (m). The main efficiencies involved in calculating the energy requirements for irrigation and their respective variations are summarized in Table 4. By taking into consideration all the aspects described in this section, in Section 3 we have analyzed the energy consumption for irrigation for the two investigated Swedish counties. Two scenarios are defined that represent the worst and best scenarios in terms of energy consumption in irrigation.

Scenario 1 (S1-energy) represents the worst scenarios in terms of energy consumption. It refers to the adoption of a sprinkler irrigation fed by a diesel-powered pump that uses groundwater as the water source. Scenario 2 (S2-energy) refers to an electrically powered micro irrigation system that pumps water from a nearby surface water source. S1 has higher energy consumption than S2 because of the higher hydraulic head (depth of water sources and required pressure for the irrigation system), higher water consumption (lower efficiency of the irrigation system), and lower pumping system efficiency (power source and pump efficiency). The parameters of those two investigated scenarios are summarized in Table 5.

2.5. Development of the visualization platform

The current version of the developed visualization platform relies on Google Earth Pro® (2021) (SWEDIMS, 2021). The model retrieves data from the SMHI models STRÅNG (2020) and MESAN (SMHI, 2020b), which are further processed with the modelling chain presented in this study. The gridded data are uploaded to the web database (SWEDIMS, 2021). Once the gridded data are stored, a parallel code develops a KMZ file to visualize the spatial data for the entire country. The generated KMZ file also allows the retrieval of time-series image data as well as MS Excel files for more than 300 locations across the country. The KMZ file was developed using the open-source package *Google Earth Toolbox* developed by Scott Lee Davis (2020).

Table 4
Summary of main efficiencies and working pressures involved in irrigation systems operation.

Parameter	Value	Reference
Irrigation system efficiency	Surface 45–80%, Sprinkler 65–90%, Micro 80–95%, Subsurface 95–98%	Irmak et al. (2011);Ehmke (2014);
Motor efficiency	40% diesel powered 90% electric powered	Daccache et al. (2014)
Pump efficiency	40–90%	Martin-Candilejo et al. (2020)
Irrigation pressure	Low Pressure 2–35 psi* Moderate Pressure 35–50 psi* Medium Pressure 50–75 psi* High Pressure 75 + psi* Surface irrigation 0 bar Drip irrigation 1 bar Sprinkler irrigation 3 bar	USDA NRCS (1997);Espinosa-Tasón et al. (2020);Daccache et al. (2014); Phocaides (2000)

*psi = pounds per square inch (1 psi = 0.7031 m of water head)

Table 5
Energy scenarios definition.

Sensitive parameter	S1-energy	S2-energy
Irrigation method	Sprinkler	Micro
Irrigation efficiency	75%	90%
Water source	Groundwater	Surface water
Power source	Diesel	Electric grid
Pump efficiency	60%	90%

3. Results and discussions

3.1. Model validation and limitations

The comparison of ET_o and crop yield using Penman–Monteith versus the Hargreaves and Samani equations is depicted in Fig. 4 (scatter plot of ET_o on the left and difference in crop yield on the right). As it shows, the Hargreaves and Samani equation slightly underestimates ET_o as compared to Penman–Monteith, as also highlighted in the study conducted by Awal et al. (2020). Nevertheless, the absolute difference in crop yield estimation is 0.11 t/ha, i.e., less than 2.5%. This result can have practical consequences in the implementation of the ET_o model, since Penman–Monteith requires significantly more input data as compared to the Hargreaves and Samani model. The validation of the simulated ET_a is presented in Fig. 5 using ET_a derived from the flux tower. The scatter plot shows an R^2 of 0.80 and RMSE of 1.38 between the derived and simulated daily ET_a during the crop-growing season using Penman–Monteith for the calculation of ET_o. The R^2 is 0.78 while the RMSE is 1.17 when the Hargreaves and Samani equation is implemented. This shows that the comparison between measured and modelled data agrees well with Zhang et al. (2016), who reported an R^2 of 0.549 between flux-tower derived ET to MODIS ET product. The relationship between the soil water content based on the daily values calculated from SWEDIMS and the values measured at the ICOS station of Lanna for different depths is presented in Fig. 6. The calculated soil water content refers to the value within the crop root depth (max. 1 m) and is based on the water balance for the grid cell of 2.5 km × 2.5 km (resolution of the gridded input data of Strång and Mesan) containing the agricultural station. Good agreement is observed between the measured and simulated values, especially with the soil water content at 0.3 m depth. It must be pointed out that, in the simulations of the soil water content, capillarity was not included. Moreover, it is worth noting two important aspects. First, the calculation of the soil water content was performed by assuming that the soil water content at the beginning of the simulations was at field capacity. Second, the field capacity is extracted by a gridded product (Global Soil Data Task Group, 2000) that cannot accurately represent the heterogeneity of soil properties at field level.

The results of the crop yield validation at the agricultural research station of Lanna are depicted in Fig. 7. The crop yield simulated with the model used in this study was compared with the crop yield retrieved from the station's principal investigator (Weslien, 2020) and Statistics Sweden (2018). The harvest at the station was approximately 5 t/ha, as reported by Weslien (2020). The oat yield from Statistics Sweden (2018) refers to the 2018 county-level oat yield in Västra Götaland County, which the Lanna research station belongs to. The simulation results in Fig. 7 show very good agreement, especially with the county-level average yield, considering that the current version of the model runs at a resolution of 2.5 km × 2.5 km and may not provide accurate crop-yield estimations at the field level due to the heterogeneity of the required input parameters. In particular, the model is sensitive to parameters such as planting date, *LAI*, and soil moisture. As Fig. 7 shows, the yield generated from the model using *LAI* data assimilation with optimization (S3-LAI) as carried out by Novelli et al. (2019) and Wagner et al. (2020) provides the most accurate results as compared to the actual measured yield. The percentage errors as compared to the

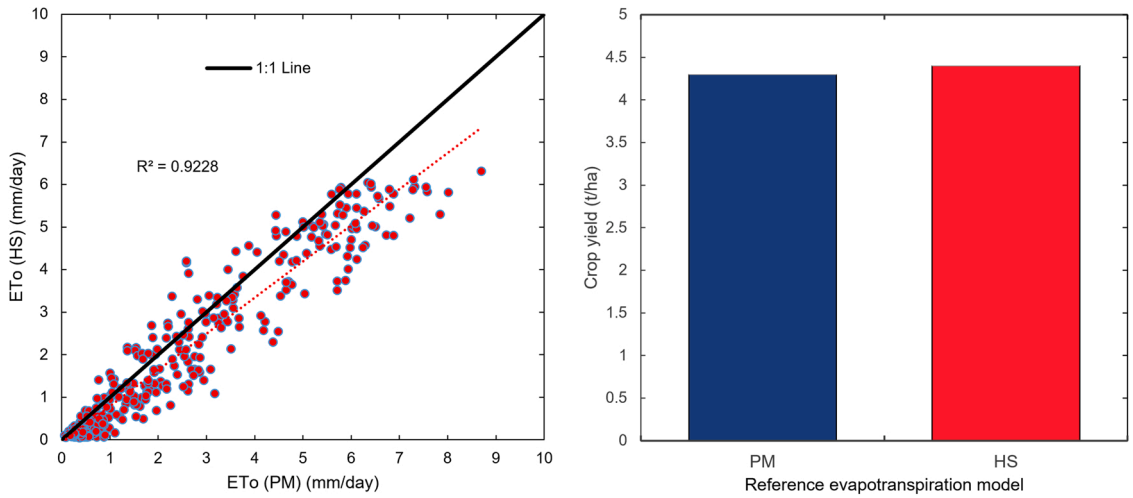

Fig. 4. Comparison between reference evapotranspiration (left) and crop yield (right) using Penman–Monteith (PM) and Hargreaves and Samani (HS) equations for 2018.

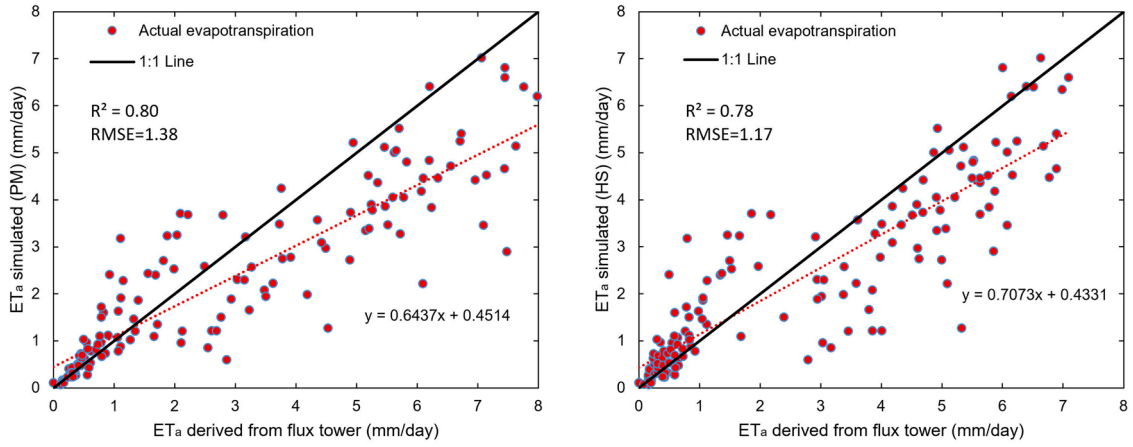

Fig. 5. Relationship between measured and calculated actual evapotranspiration using Penman–Monteith (PM) and Hargreaves and Samani (HS) equations for 2018 during the crop-growing season. The measured data was from Lanna ICOS station in 2018.

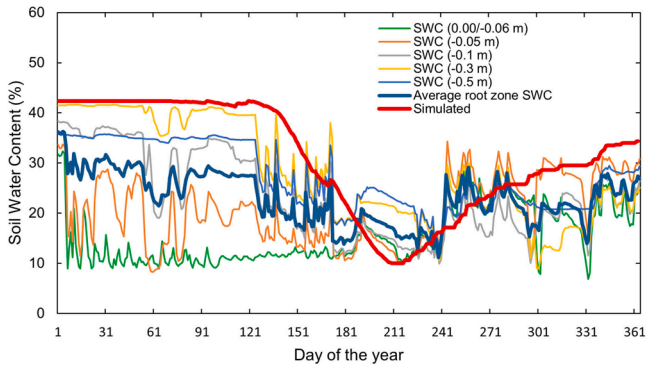

Fig. 6. Measured soil water content at different depths at Lanna ICOS station and calculated soil water content within crop root depth for 2018.

measured crop yield and the county-level statistics are 2% and 10.6%, respectively. Those results agree with results presented by Wagner et al. (2020) that demonstrated the superiority of the optimization method as compared to simple updating. The authors also demonstrated that the optimization approach could lead to similar or even improved results as compared to more advanced data assimilation algorithms, such as extended Kalman filter updating. The *LAI* curve after optimization of the shape key parameters and the *LAI* data from CGLS are depicted in Fig. 8. The crop-yield simulations using the default crop parameters as in Williams et al. (1989) show similar results as providing simple updates of *LAI* values from CGLS (Fig. 7). Similar accurate results could be obtained by updating the planting date using the values reported in Morel et al. (2021). The *LAI* data from CGLS comes with a five-day delay. In an operational system, this could lead to some inaccuracies in estimating water use for irrigation and crop yield (i.e., the potential biomass accumulation). This aspect is not investigated in this study but will be assessed in future experimental studies. Balkovič et al. (2013) reported similar yields for oat in their comprehensive EPIC multi-crop simulation across Europe. Foltescu (2000) also reported similar yields by running the WOFOST crop model using MESAN climatological parameters as input.

The ET_a and soil moisture models' validation has been performed only at one location and for one crop for 2018. The ICOS network, that provides open-source data, had only one flux tower on agricultural land in Sweden (https://www.icos-sweden.se/Lanna) in 2018. Currently, that flux tower has been closed at the end of 2020 (the current operating stations can be found at https://www.icos-sweden.se/stations). Other flux towers belonging to the ICOS network are installed on other type of ecosystems such as wetland and forest. To make up for the lack of data, our research group is establishing an experimental facility where we

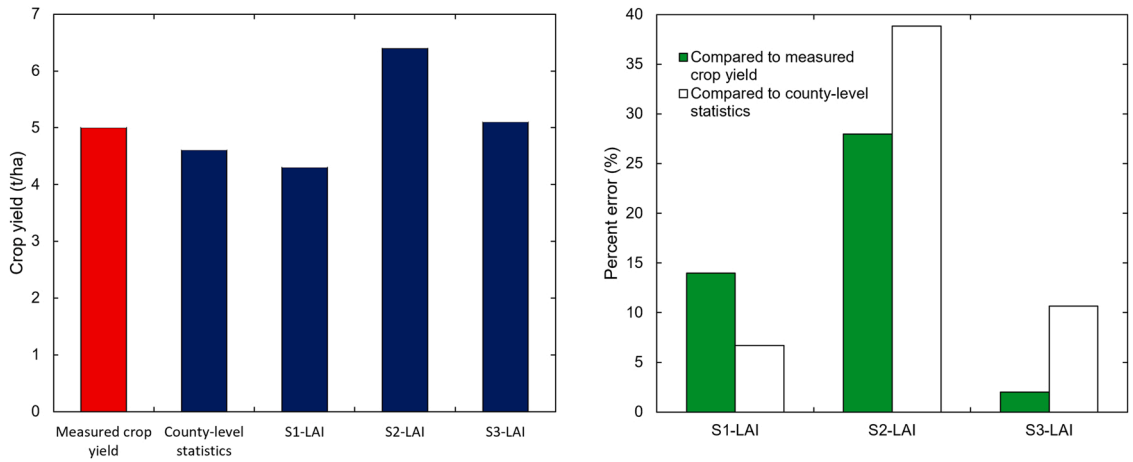

Fig. 7. Crop yield validation for 2018.

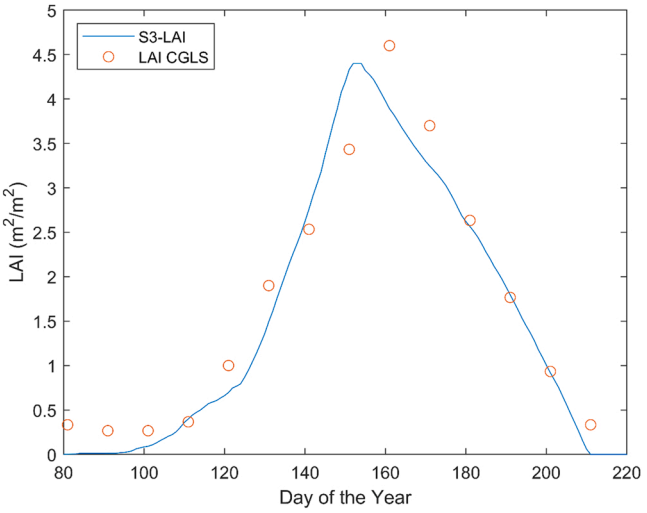

Fig. 8. Time series of assimilated leaf area index and Copernicus Global Land Service (CGLS) leaf area index observations for 2018.

compare crop yields in open field conditions as well under agrivoltaic systems. This is connected to the project "*Evaluation of the first agrivoltaic system in Sweden*" (Mälardalen University, 2022). In future studies, we will use the data gathered by the monitoring system, including distributed soil moisture and temperature sensors and micro-lysimeters, and crop yield experiments to further validate the model presented in this study.

3.2. Irrigation water productivity and crop model validation

The results of the *IWP* (kg/m^3) for the investigated irrigation scenarios are summarized in Fig. 9 for 2018 and in Fig. 10 for 2019. The irrigation guidelines provided by the model developed in this study show the highest values of *IWP* in most of the considered grids for both 2018 and 2019. The scenarios S2-irrigation static 100 and S3-irrigation static 150 derived from Bergström and Barkefors (2004) and from the Swedish Board of Agriculture (2007) show lower *IWP* values both in 2018 and 2019. As compared to scenarios S2 and S3-irrigation, the guidelines provided by the developed spatially explicit model show higher water volumes for irrigation (i.e., negative water savings in Fig. 11), but maintain higher *IWP* values in most of the grids, as Fig. 9 shows.

In 2018, the proposed irrigation management system could lead to water savings mostly of between −75% and −40% as compared to S2-irrigation static 100 and of between −55% and −10% as compared to S3-irrigation static 150 as depicted in Fig. 11 (left). Nevertheless, by analyzing the crop yield increase of scenario S1-irrigation ET as compared to scenarios S2-irrigation static 100 and S3-irrigation static 150 (see Fig. 11 [right]), it can be easily noted that crop yield increase from the proposed irrigation management system vary between 10% and 60% as compared to conventional irrigation guidelines. Most of the input data for irrigation management vary temporally and spatially, making spatially explicit guidelines fundamental. Meanwhile, with intensifying climate changes and more frequent extreme weather events in recent years, such as the severe drought of 2018, it becomes more difficult to apply "typical meteorological" year guidelines based on past experiences (Melton et al., 2012). By analyzing the results concerning water savings and crop yield increase for 2019 (a more "typical meteorological" year as compared to 2018) depicted in Fig. 12, we see that most of the water savings range between −20% and 80% as compared to scenario S2-irrigation static 100 and between 20% and 100% as compared to scenario S3-irrigation static 150. Even in 2019, by assuming static guidelines, the crop yield increase of scenario S1-irrigation ET ranges between −5–30% as compared to the scenarios based upon conventional irrigation guidelines. Those modelling results align with the results from Johnson et al. (2016).

A further model run for scenario S1-irrigation ET was performed using a threshold K_s value of 0.6 (i.e., irrigation is performed only when the water stress coefficient reaches a value of 0.6). The results are summarized in Fig. 13. As can be seen, scenario S1-irrigation ET and scenario S3-irrigation static 150 suggest similar applied irrigation volumes (e.g., the irrigation volumes for S1-irrigation ET are mostly distributed between 100 and 160 mm); nevertheless, the resulting crop yields for scenario S1-irrigation ET are significantly higher than for Scenario S3-irrigation due to better irrigation scheduling. This further support the superiority of spatially explicitly ET_c-driven guidelines as compared to conventional non-spatially- and non-temporally-driven irrigation guidelines. ET_c-driven irrigation was also acknowledged by Ko and Piccinni (2009) as one of the efficient irrigation schemes for achieving higher water-use efficiency for growing corn in Texas. Similar, Hanson and Putnam (2000) pointed out that water consumption in irrigation for Alfalfa in California can be reduced through improved irrigation scheduling by considering dynamic variation of ET_c and soil moisture. The authors also investigated the effects of deficit irrigation and pointed out that further water savings in irrigation can be achieved by reducing or avoiding irrigation during those periods when the crop yield per water applied is minimal. Similar conclusions for maximizing Alfalfa water-use efficiency in the Great Plains and Intermountain were achieved by Lindenmayer et al. (2011).

In 2018, the crop yield reduction due to temperature stress was up to

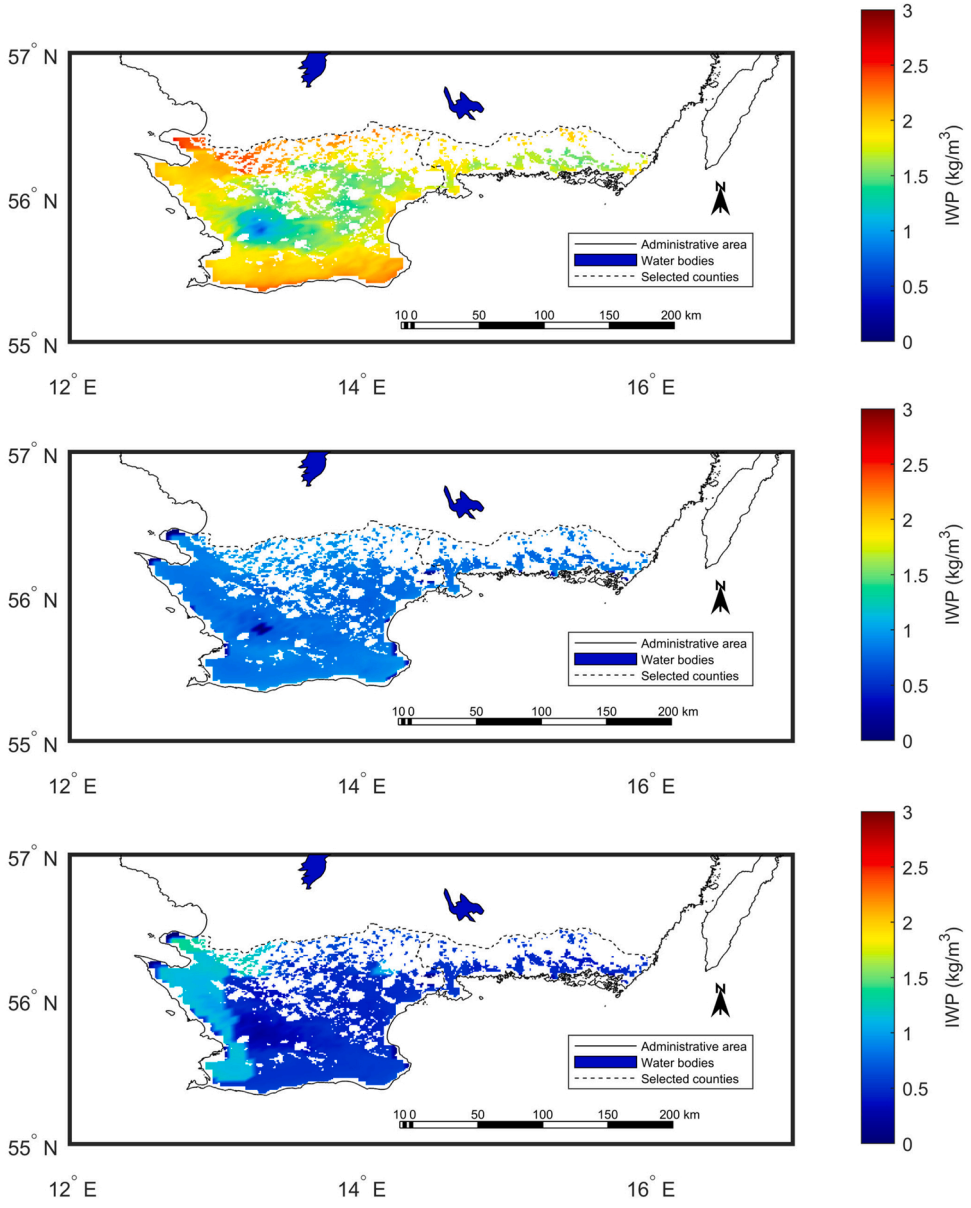

Fig. 9. Irrigation water productivity (IWP) (according to guidelines from SWEDIMS [S1-irrigation ET] [top], S2-irrigation static 100 [center], and S3-irrigation static 150 [bottom]) in 2018.

30% as compared to the ideal case without temperature stress as depicted in Fig. 14. The results refer to two cases: no irrigation and S1-irrigation ET. Since the WFE nexus also represents a framework for innovations and technologies for sustainable natural resources management, an important technology that could be integrated in the agricultural and irrigation sector to reduce the impacts of water and temperature stresses on crops is agrivoltaic (i.e., the combination of photovoltaic systems and crop production in the same area). Agrivoltaic systems, as well as photovoltaic water pumping systems for irrigation, can simultaneously address the interactions among water, energy, and food. Due to shade cast on crops, Amaducci et al. (2018) demonstrated that agrivoltaic systems with an optimal density of PV modules can increase crop yields due to their ability to maintain higher levels of soil moisture in Italy. Similarly, Barron-Gafford et al. (2019) showed that the combination of PV systems with farm activities could lead to reduced drought impact and higher food yield in Arizona. At high latitudes like in Sweden, the tradeoffs between water and temperature stresses reductions, which can lead to increased crop yields, and *PAR* reductions due to the shadings produced by the PV modules, which can negatively affect crop yields, are worth of investigations. The models and frameworks developed in this study combined with the optimization model for agrivoltaic systems presented in Campana et al. (2021) can be a starting point to investigate the effects deployment of agrivoltaic systems to support the irrigation sector on large-scale.

The validation of the potatoes crop model for the selected counties in Sweden is presented in Figs. 15–16 for 2018 and 2019, respectively, using county-level statistics (Statistics Sweden, 2022b). We have assumed a 20% dry matter weight to reconcile fresh matter and dry matter data. Both for 2018 and 2019, the statistics available for Skåne and Blekinge concerning the average potato yield are comprised between the average crop yield simulated under no irrigation and irrigation scenarios. The variation between crop yield under the no irrigation and irrigation scenarios is significantly reduced in 2019 as compared to 2018 due the absence of an extreme weather phenomena hitting the region. Those last results confirm the robustness of the model. Unfortunately, in Sweden, only county-level statistics are available, and no statistics differentiate between irrigated and non-irrigated crop yields, as for instance in the United States of America (USDA, 2022). More

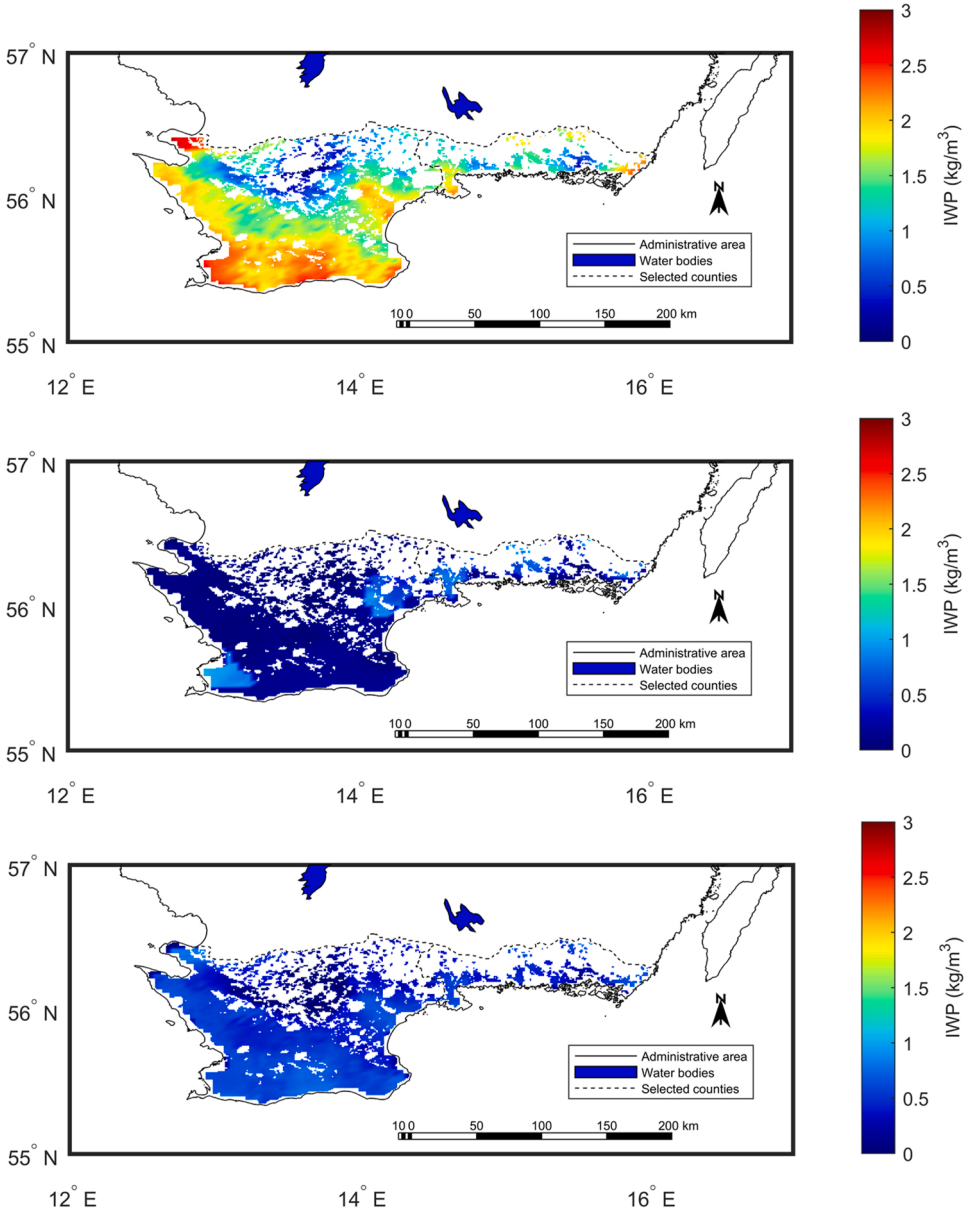

Fig. 10. Irrigation water productivity (IWP) (according to guidelines from SWEDIMS [S1-irrigation ET] [top], S2-irrigation static 100 [center], and S3-irrigation static 150 [bottom]) in 2019.

detailed statistics and methods like IrrMapper (Ketchum et al., 2020), a machine learning based model for mapping irrigation-status at high spatial resolution, could be used to further validate the simulated crop yield at county or sub-county levels for irrigated and non-irrigated areas. The potential crop yields under irrigation regimes also agrees with the values reported in Ekelöf et al. (2015), Zhou et al., (2016, 2018), and Jennings et al. (2020).

3.3. Energy consumption and further developments

Energy consumptions in the irrigation sector for the different scenarios as defined in Table 5 are depicted in Figs. 17 and 18. The scenario S1-energy shows an energy consumption in the order of ten times higher than the best-case scenario (S2-energy). This is due to the combination of efficiencies in the modelling chain, water resources depth, and other parameters (see Table 5). While these results might not significantly affect a single farmer due to the current low electricity prices in Sweden (Eurostat, 2021), it might substantially affect the regional energy systems in terms of matching electricity supply and demand. This mismatch at a larger scale (i.e., not at farm level but on a regional level) might lead to spikes in the electricity prices due to higher demands that can afterwards affect farmers and, more generally, all the electricity buyers. Moreover, this is likely to happen during extreme droughts events and or for long-term negative climate changes that typically put pressure on energy systems, in particular on hydropower and thermal energy conversion plants (Riksbanken, 2018). From a WFE nexus perspective, the results in Figs. 17 and 18 are important in broader energy and water contexts. To better understand the WFE nexus with an integrated approach, the model presented in this study will be further developed to analyze other key sectors, such as the agricultural sector as a whole (i.e., not only the irrigation sector as in this study), industrial, power, commercial, and residential sectors. The developed model will be able to study spatially explicit water and energy demand and supply at high temporal resolution, which will enable the identification of potential energy demand and supply mismatches, especially during extreme events and/or using climate change scenarios data. The

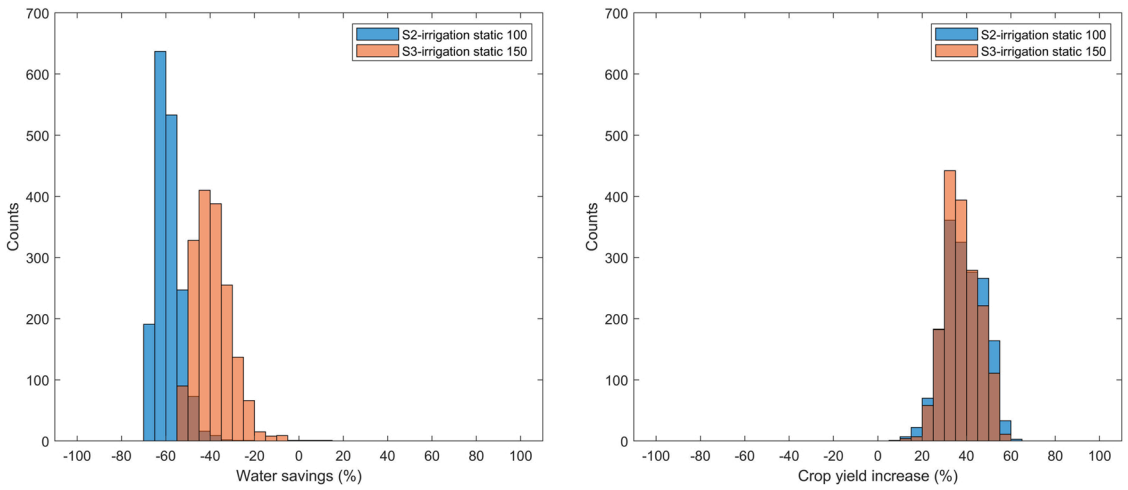

Fig. 11. Water savings using irrigation guidelines from the developed model (scenario S1-irrigation ET) versus scenarios S2-irrigation static 100 and S3-irrigation static 150 (left); and crop yield increase of scenario S1-irrigation ET versus scenarios S2-irrigation static 100 and S3-irrigation static 150 (right), for 2018.

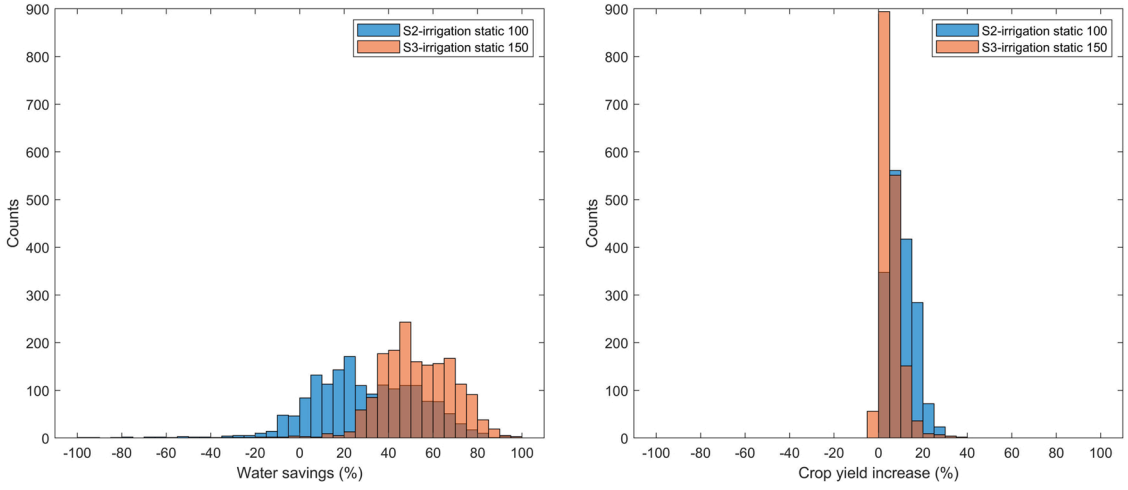

Fig. 12. Water savings using irrigation guidelines from the developed model (scenario S1-irrigation ET) versus scenarios S2-irrigation static 100 and S3-irrigation static 150 (left); and crop yield increase of scenario S1-irrigation ET versus scenarios S2-irrigation static 100 and S3-irrigation static 150 (right), for 2019.

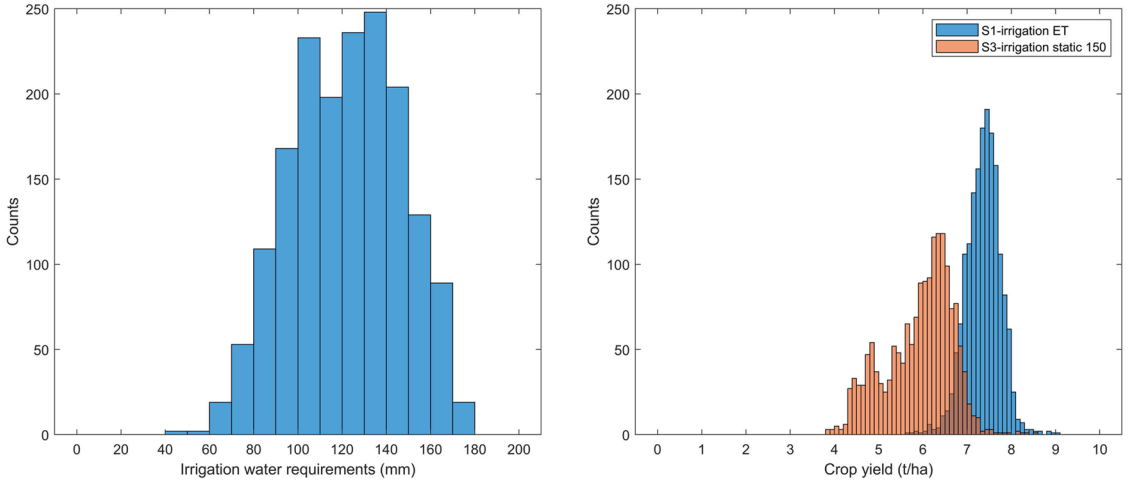

Fig. 13. Comparison between scenario S1-irrigation ET and S3-irrigation static 150 in terms of irrigation water requirements (mm) (left) (the distribution refers only to scenario S1-irrigation ET since for scenario S3-irrigation static 150 the irrigation water requirements for each investigated grid point is 150 mm) and corresponding crop yield (right). Scenario S1-irrigation ET is obtained by using a water stress coefficient threshold of 0.6.

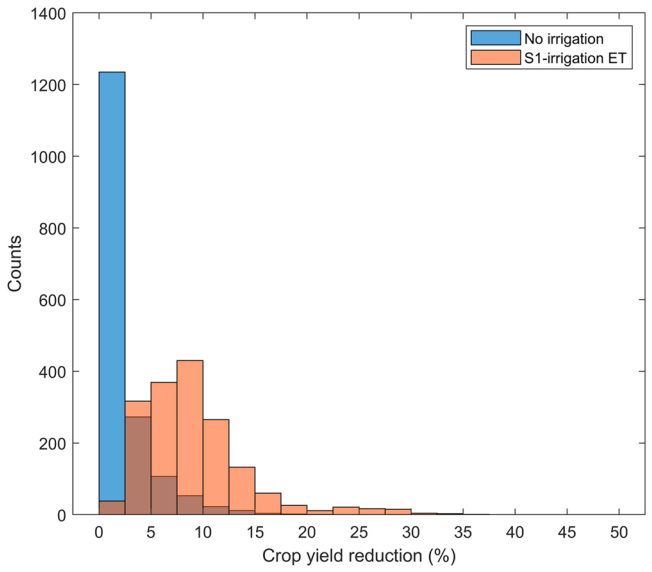

Fig. 14. Crop yield reduction due to temperature stress for no irrigation and for scenario S1-irrigation ET in 2018.

integration of such a model with a hydrological model will also allow to identify potential water supply and demand mismatches, spatially and temporally, and thus better allocate water resources.

3.4. The irrigation management service interface

A screenshot of the demonstrator for the irrigation management service interface is provided in Fig. 19, where the users can view the daily ET_o maps for all of Sweden. Once all the data are retrieved from the server, the maps can be visualized with a time dimension by using the time slider. By specifying the field *Evapotranspiration cities*, the users can also view and download daily-based time series of ET_o and precipitation data for the selected locations across the country (Fig. 20). The locations for which it is possible to retrieve the ET_o and precipitation time series appear on the map. The data on ET_o and precipitation can be used as a starting point for more accurate assessment of specific crop water requirements using the FAO guidelines (Allen et al., 1998). Moreover, by assimilating *LAI* observations as described in Sections 2.2 and 3.1 and other satellite derived parameters, the current version of the model could be further expanded to specifically cover the most irrigated crops in the country, providing timely guidelines for farmers. By integrating ET_o maps with maps of irrigation areas and water resource depths and availabilities, water- and energy-management agency managers could have a better view of potential water and energy consumption from the irrigation sector. The developed interface demonstrator can provide large-scale and cost-effective irrigation management services and decision support in both developed and developing countries, especially in those areas with significant water and food security issues.

4. Conclusions

This study aimed to develop a demonstrator of operational

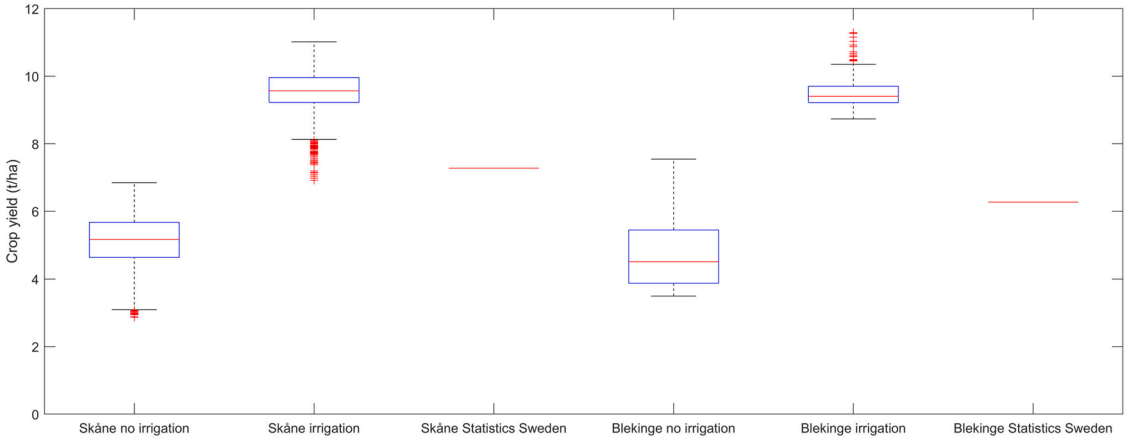

Fig. 15. Crop model validation using county level statistics (Statistics Sweden, 2022b) for 2018.

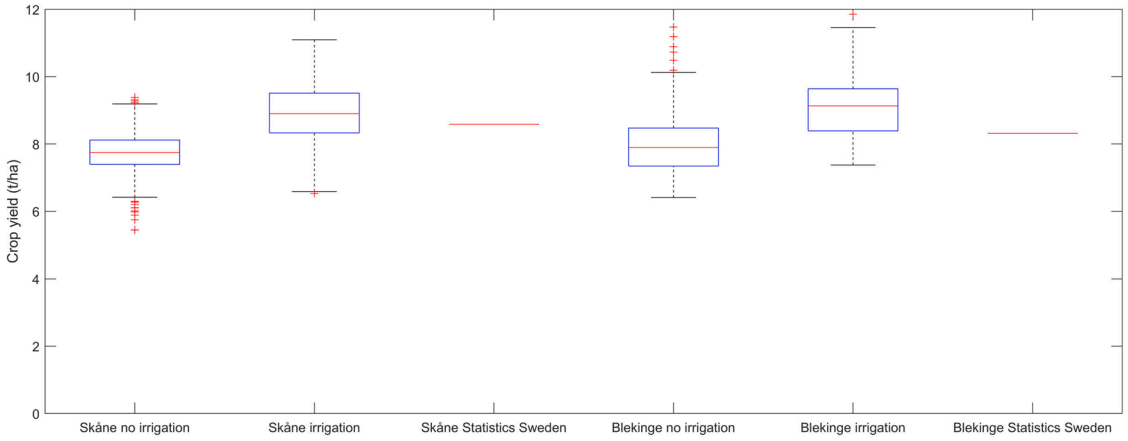

Fig. 16. Crop model validation using county level statistics (Statistics Sweden, 2022b) for 2019.

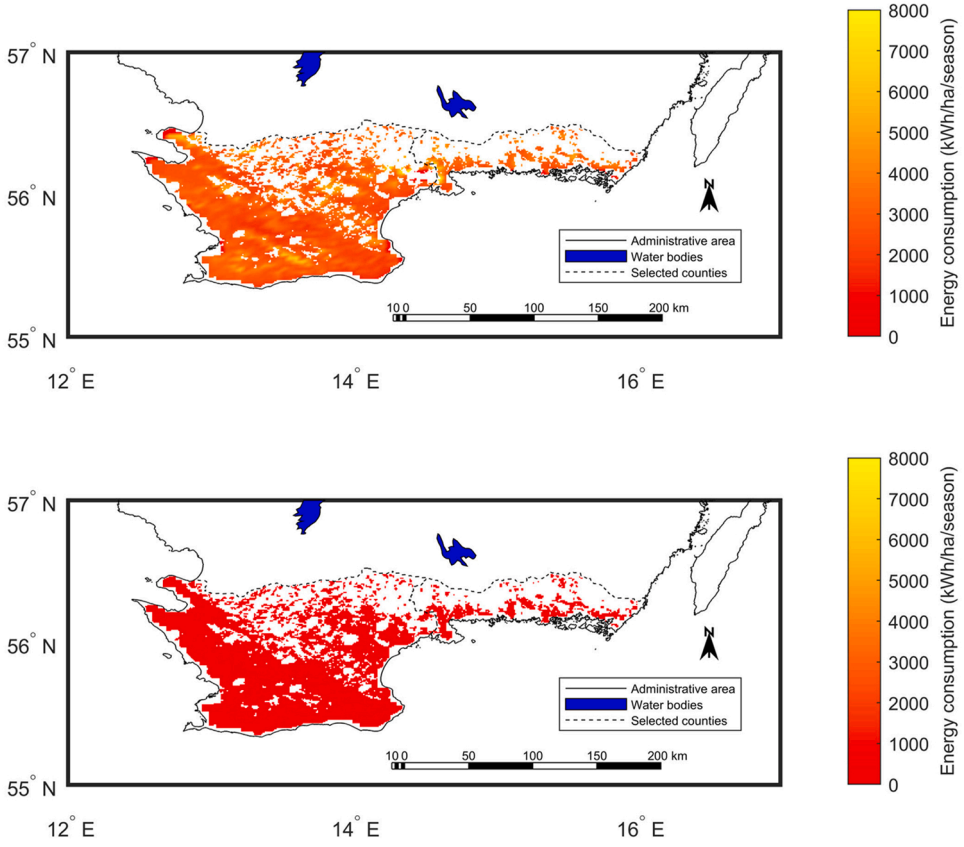

Fig. 17. Comparison between energy consumption in the irrigation sector in the investigated worst-case (S1-energy) (top) and best-case (S2-energy) (bottom) scenarios.

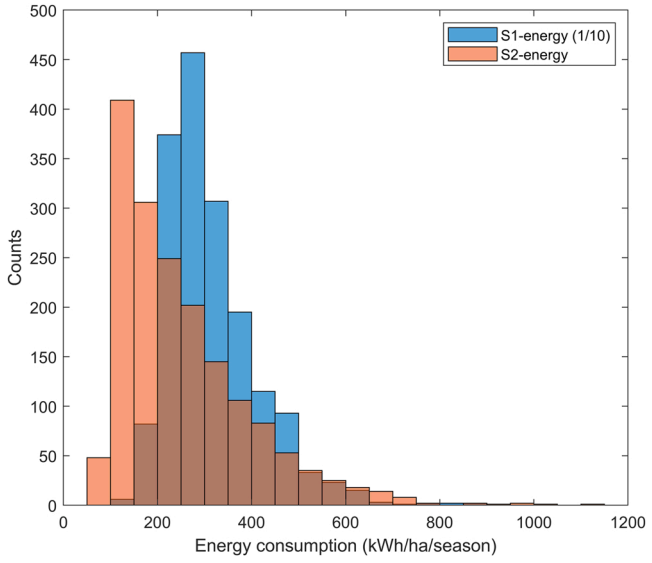

Fig. 18. Distribution of energy consumption in the irrigation sector in the investigated worst (S1-energy) and best (S2-energy) energy scenarios.

water–food–energy nexus system for the irrigation sector in Sweden, focusing on the interrelationships between water and energy requirements for irrigation and corresponding crop yield response. The 2018 drought that severely hit Sweden is used as the case study. The results are compared with 2019, a more "typical meteorological" year as compared to 2018. The main conclusions from this study are the following:

- The use of the Penman–Monteith equation instead of the Hargreaves and Samani equation for estimating the crop reference evapotranspiration shows slightly better results in the modelling chain for estimating oats yield: 0.11 t/ha difference at Lanna in 2018. Despite the higher performances of Penman–Monteith equation, it requires significantly more input data as compared to the Hargreaves and Samaniś model. This demonstrates that the implementation of Hargreaves and Samani equation could provide a good trade-off between accuracy and complexity for an operational service.
- By assimilating through optimization the leaf area index from Copernicus Global Land Service into the crop model, the model presents the best results while comparing the simulated crop yield with the measured crop yield at the Lanna ICOS station.
- The irrigation water productivity using the developed model shows better results as compared to irrigation scenarios based on existing static and non-spatially explicit guidelines both in 2018 and in 2019.
- During the drought year 2018, the developed model showed no irrigation water savings as compared to conventional irrigation guidelines. Nevertheless, the crop yield increase from the proposed irrigation management system varied between 10% and 60% as compared to conventional irrigation guidelines.
- In 2019, most of the water savings ranged between −20% (i.e., increased irrigation water volume as compared to static guidelines) and 80%, with crop yield increases ranging between −5% (i.e., decreased crop yield) and 30%. Those modelling results align with previous studies on implementing large-scale irrigation management services in the United States of America.
- The modelling result shows a significant reduction in crop yield of up to 30% due to temperature stress as compared to the ideal case in which temperature stress is absent. This, connected to the high water stress in 2018, might justify the implementation of technologies that

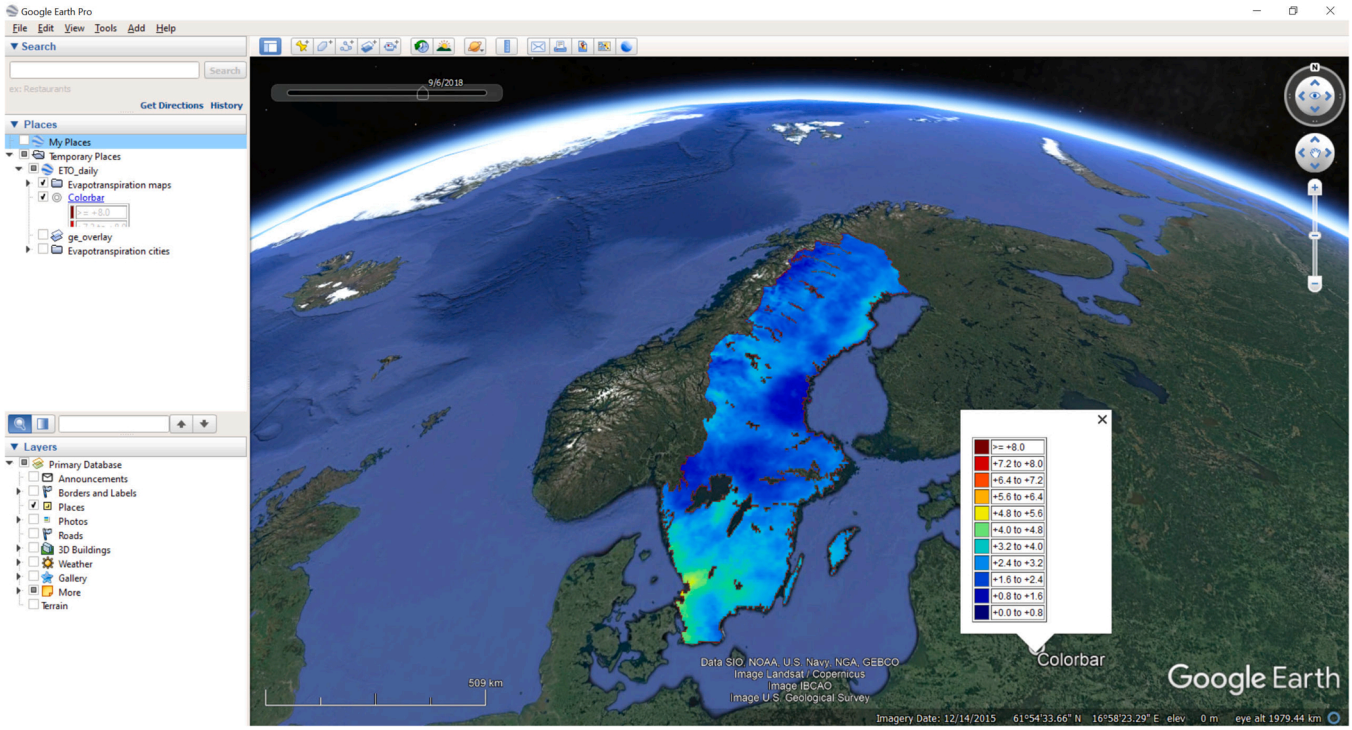

Fig. 19. Screenshot of the demonstrator for the irrigation management service interface.

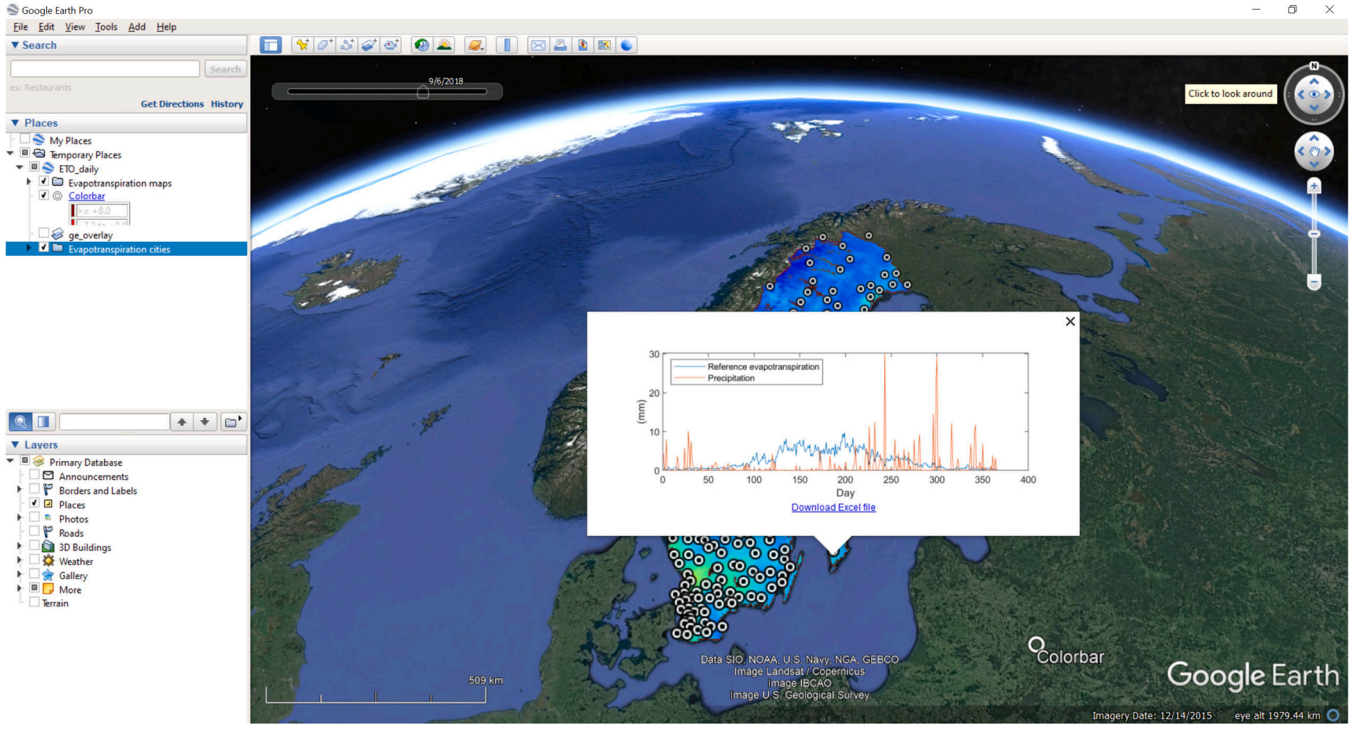

Fig. 20. Retrieval of time-series reference evapotranspiration and precipitation for a specified location.

can mitigate the negative effects of weather extremes (e.g., drought) and climate changes on water–food–energy nexus interrelationships.

- The developed demonstrator, based on an open-source package for Google Earth®, can be easily implemented to help farmers and water- and energy-management agencies to better understand the water, energy, and food interrelationships and make informed decisions, especially during the occurrence of extreme events.
- The developed demonstrator interface can provide large-scale and cost-effective irrigation management services and decision support in both developed and developing countries.

In future studies, the proposed model will be extended to other key sectors, such as the power and industrial sector, to support the optimal large-scale allocation of water and natural resources.

Declaration of Competing Interest

The authors declare that they have no known competing financial interests or personal relationships that could have appeared to influence the work reported in this paper.

Acknowledgements

The authors acknowledge ICOS for provisioning the data from the Lanna station to validate the models of crop yield, actual evapotranspiration, and soil moisture. The authors would like to thank Per Weslien for assistance. ICOS Sweden is funded by the Swedish Research Council as a national research infrastructure. Pietro Elia Campana acknowledges the Future Energy Center internal funding for the projects "Towards An Optimal Irrigation Management System from the Water–Food–Energy Nexus Perspective" and "A Gridded Water–Food–Energy Nexus Management System for Sweden", the Swedish Energy Agency for the project "Evaluation of the first agrivoltaic system in Sweden" (grant number 51000–1), and Formas - the Swedish Research Council for Sustainable Development, for the funding received through the early career project "Avoiding conflicts between the sustainable development goals through agro-photovoltaic systems" (grant number FR-2021/0005). Pietro Elia Campana also thanks the financial support from Almi for the computing facilities. The support received from Mattias Holmquist, coordinator of the biosphere area Blekinge Arkipelag, is sincerely appreciated.

References

Allen, R.G., Pereira, L.S., Raes, D., Smith, M., 1998. Crop evapotranspiration-Guidelines for computing crop water requirements-FAO Irrigation and drainage, 300. FAO, Rome.
Amaducci, S., Yin, X., Colauzzi, M., 2018. Agrivoltaic systems to optimise land use for electric energy production. Appl. Energy 220, 545–561.
Awal, R., Habibi, H., Fares, A., Deb, S., 2020. Estimating reference crop evapotranspiration under limited climate data in West Texas. J. Hydrol.: Reg. Stud. 28, 100677.
Balkovič, J., van der Velde, M., Schmid, E., Skalský, R., Khabarov, N., Obersteiner, M., Xiong, W., 2013. Pan-European crop modelling with EPIC: Implementation, up-scaling and regional crop yield validation. Agric. Syst. 120, 61–75.
Barron, J. (2020, June 3). Personal interview.
Barron-Gafford, G.A., Pavao-Zuckerman, M.A., Minor, R.L., Sutter, L.F., Barnett-Moreno, I., Blackett, D.T., Macknick, J.E., 2019. Agrivoltaics provide mutual benefits across the food–energy–water nexus in drylands. Nat. Sustain. 2 (9), 848–855.
Battilani, A. (2004, November). Fertirrigere V2. 11: a multi-target DSS to manage water and nutrient supply at macrozone level. In IX International Symposium on the Processing Tomato 724 (pp. 111–118).
Bazilian, M., Rogner, H., Howells, M., Hermann, S., Arent, D., Gielen, D., Yumkella, K.K., 2011. Considering the energy, water and food nexus: towards an integrated modelling approach. Energy Policy 39 (12), 7896–7906.
Belusic, D., Berg, P., Bozhinova, D., Bärring, L., Doescher, R., Eronn, A., Strandberg, G., 2019. Clim. Extrem. Swed. https://doi.org/10.17200/Climate_Extremes_Sweden.
Bergström, U., & Barkefors, C. (2004). Irrigation in dose assessments models (No. SKB-R–04–26). Swedish Nuclear Fuel and Waste Management Co.
Bioenergy International. Available at: ⟨https://bioenergyinternational.com/feedstock/swedens-2018-crop-harvest-worst-since-the-late-1950s⟩. Accessed 24th August 2020.
Bos, M.G. (1985). Summary of ICID definitions on irrigation efficiency.
Brundell, P., Kanlén, F., Westöö, A.K., 2008. Water use for irrigation. Rep. Grant Agreem., (71301. 2006) 002–2006.
Campana, P.E., Li, H., Zhang, J., Zhang, R., Liu, J., Yan, J., 2015. Economic optimization of photovoltaic water pumping systems for irrigation. Energy Convers. Manag. 95, 32–41.
Campana, P.E., Stridh, B., Amaducci, S., Colauzzi, M., 2021. Optimisation of vertically mounted agrivoltaic systems. J. Clean. Prod. 325, 129091.
Campana, P.E., Zhang, J., Yao, T., Andersson, S., Landelius, T., Melton, F., Yan, J., 2018. Managing agricultural drought in Sweden using a novel spatially-explicit model from the perspective of water-food-energy nexus. J. Clean. Prod. 197, 1382–1393.
Copernicus Global Land Service. Available at: ⟨https://land.copernicus.eu/global/products/lai⟩. Accessed 17th October 2020.
Daccache, A., Ciurana, J.S., Diaz, J.R., Knox, J.W., 2014. Water and energy footprint of irrigated agriculture in the Mediterranean region. Environ. Res. Lett. 9 (12), 124014.
Dai, J., Wu, S., Han, G., Weinberg, J., Xie, X., Wu, X., Yang, Q., 2018. Water-energy nexus: a review of methods and tools for macro-assessment. Appl. Energy 210, 393–408.
Deb, K., Agrawal, S., Pratap, A., & Meyarivan, T. (2000, September). A fast elitist non-dominated sorting genetic algorithm for multi-objective optimization: NSGA-II. In International conference on parallel problem solving from nature (pp. 849–858). Springer, Berlin, Heidelberg.
DeJonge, K.C., Ascough J.C., Ii, Andales, A.A., Hansen, N.C., Garcia, L.A., Arabi, M., 2012. Improving evapotranspiration simulations in the CERES-Maize model under limited irrigation. Agric. Water Manag. 115, 92–103.
Dominic, W. (2011). Water Security: The Water-Food-Energy-Climate Nexus: The World Economic Forum Water Initiative.
Ehmke, T., 2014. Subsurface drip irrigation: battling drought, water restrictions, and declining groundwater. Crops Soils 47 (4), 4–10.
Ekelöf, J., Guamán, V., Jensen, E.S., Persson, P., 2015. Inter-row subsoiling and irrigation increase starch potato yield, phosphorus use efficiency and quality parameters. Potato Res. 58 (1), 15–27.
Endo, A., Yamada, M., Miyashita, Y., Sugimoto, R., Ishii, A., Nishijima, J., Kumazawa, T., 2019. Dynamics of water–energy–food nexus methodology, methods, and tools. Curr. Opin. Environ. Sci. Health.
Espinosa-Tasón, J., Berbel, J., Gutiérrez-Martín, C., 2020. Energized water: evolution of water-energy nexus in the spanish irrigated agriculture, 1950–2017. Agric. Water Manag. 233, 106073.
Eurostat. (2021) Available at: ⟨https://ec.europa.eu/eurostat/statistics-explained/index.php/Electricity_price_statistics#Electricity_prices_for_non-household_consumers⟩. Accessed 31st January 2021.
Fan, Y., Li, H., Miguez-Macho, G., 2013. Global patterns of groundwater table depth. Science 339 (6122), 940–943.
Foltescu, V.L., 2000. Prediction of crop yield in Sweden based on mesoscale meteorological analysis. Meteorol. Appl.: A J. Forecast., Pract. Appl., Train. Tech. Model. 7 (4), 313–321.
Food and Agriculture Organization (2016). AQUASTAT: Global map of irrigation areas.
Food and Agriculture Organization (2017). The Future of Food and Agriculture: Trends and Challenges.
FutureWater. Available at: ⟨https://www.futurewater.eu/projects/irrigation-management-romania/⟩. Accessed 30th January 2020.
Galindo, J., Torok, S., Salguero, F., de Campos, S., Romera, J., Puig, V., 2017. Optimal management of water and energy in irrigation systems: application to the bardenas canal. IFAC-Pap. 50 (1), 6613–6618.
Gallardo, et al., 2020. Decision support systems and models for aiding irrigation and nutrient management of vegetable crops. Agric. Water Manag. 106209.
Global Soil Data Task Group. 2000. Global Gridded Surfaces of Selected Soil Characteristics (IGBP-DIS).
Google Earth Pro®. Available at: ⟨https://www.google.com/earth/versions/⟩. Accessed 9th January 2021.
Gorelick, N., Hancher, M., Dixon, M., Ilyushchenko, S., Thau, D., Moore, R., 2017. Google earth engine: planetary-scale geospatial analysis for everyone. Remote Sens. Environ. 202, 18–27.
Government Offices of Sweden, The agricultural sector and the drought, ⟨https://www.government.se/articles/2018/08/the-agricultural-sector-and-the-drought/⟩. Accessed 24th May 2020.
Grusson, Y., Wesström, I., Joel, A., 2021a. Impact of climate change on Swedish agriculture: growing season rain deficit and irrigation need. Agric. Water Manag. 251, 106858.
Grusson, Y., Wesström, I., Svedberg, E., Joel, A., 2021b. Influence of climate change on water partitioning in agricultural watersheds: examples from Sweden. Agric. Water Manag. 249, 106766.
Grusson, Y., Barron, J. (2021c). Challenges In Reanalysis Products To Assess Extreme Weather Impacts On Yield Underestimate Drought. ⟨10.21203/rs.3.rs-908090/v1⟩.
Gu, L., Hu, Z., Yao, J., Sun, G., 2017. Actual and reference evapotranspiration in a cornfield in the zhangye oasis, northwestern China. Water 9 (7), 499.
Hanson, B., & Putnam, D. (2000, December). Can alfalfa be produced with less water. In Proc. 29th Natl. Alfalfa Symp. and 30th California Alfalfa Symp (pp. 00–043). Davis, CA: Univ. CA, Dept. of Agronomy and Range Science.
Hargreaves, G.H., Samani, Z.A., 1982. Estimating potential evapotranspiration. J. Irrig. Drain. Div. 108 (3), 225–230.
ICOS. (2019). Ecosystem Thematic Centre and Lanna: Drought-2018 ecosystem eddy covariance flux product from Lanna, doi:⟨10.18160/GPS8-BGNW⟩.
ICOS. (2021). Available at: ⟨https://www.icos-sweden.se/lanna⟩.
IRMA_SYSTEM. (2021). Available at: ⟨https://arta.interregir2ma.eu/⟩.
Irmak, S., Odhiambo, L.O., Kranz, W.L., & Eisenhauer, D.E. (2011). Irrigation efficiency and uniformity, and crop water use efficiency.
Jennings, S.A., Koehler, A.K., Nicklin, K.J., Deva, C., Sait, S.M., Challinor, A.J., 2020. Global potato yields increase under climate change with adaptation and CO_2 fertilisation. Front. Sustain. Food Syst. 248.
Jin, X., Kumar, L., Li, Z., Feng, H., Xu, X., Yang, G., Wang, J., 2018. A review of data assimilation of remote sensing and crop models. Eur. J. Agron. 92, 141–152.
Johnson, L.F., Cahn, M., Martin, F., Melton, F., Benzen, S., Farrara, B., Post, K., 2016. Evapotranspiration-based irrigation scheduling of head lettuce and broccoli. HortScience 51 (7), 935–940.
Jungqvist, G., Oni, S.K., Teutschbein, C., Futter, M.N., 2014. Effect of climate change on soil temperature in Swedish boreal forests. PloS One 9, 4.
Kaddoura, S., El Khatib, S., 2017. Review of water-energy-food Nexus tools to improve the Nexus modelling approach for integrated policy making. Environ. Sci. Policy 77, 114–121.
Ketchum, D., Jencso, K., Maneta, M.P., Melton, F., Jones, M.O., Huntington, J., 2020. IrrMapper: a machine learning approach for high resolution mapping of irrigated agriculture across the Western US. Remote Sens. 12 (14), 2328.
Ko, J., Piccinni, G., 2009. Corn yield responses under crop evapotranspiration-based irrigation management. Agric. Water Manag. 96 (5), 799–808.
Konak, A., Coit, D.W., Smith, A.E., 2006. Multi-objective optimization using genetic algorithms: a tutorial. Reliab. Eng. Syst. Saf. 91 (9), 992–1007.

Krikken, F., Lehner, F., Haustein, K., Drobyshev, I., van Oldenborgh, G.J., 2019. Attribution of the role of climate change in the forest fires in Sweden 2018. Nat. Hazards Earth Syst. Sci. Discuss. 1–24.
Lawford, R.G., 2019. A design for a data and information service to address the knowledge needs of the Water-Energy-Food (WEF) Nexus and strategies to facilitate its implementation. Front. Environ. Sci. 7, 56.
Lindenmayer, R.B., Hansen, N.C., Brummer, J., Pritchett, J.G., 2011. Deficit irrigation of alfalfa for water-savings in the Great Plains and Intermountain West: a review and analysis of the literature. Agron. J. 103 (1), 45–50.
Liu, J., Yang, H., Cudennec, C., Gain, A.K., Hoff, H., Lawford, R., Qi, J., de Strasser, L., Yillia, P.T., Zheng, C., 2017. Panta Rhei Opinions: challenges in operationalizing the water-energy-food nexus. Hydrol. Sci. J. 62 (11), 1714–1720.
Mahmoud, S.H., Gan, T.Y., 2019. Irrigation water management in arid regions of Middle East: assessing spatio-temporal variation of actual evapotranspiration through remote sensing techniques and meteorological data. Agric. Water Manag. 212, 35–47.
Malamos, N., Tsirogiannis, I.L., Christofides, A., Anastasiadis, S., Vanino, S., 2015. Main features and application of a web-based irrigation management tool for the plain of Arta (September). HAICTA 174–185.
Mälardalen University. (2022). Evaluation of the first agrivoltaic system in Sweden. Available at: ⟨https://www.mdu.se/en/malardalen-university/research/research-projects/evaluation-of-the-first-agrivoltaic-system-in-sweden⟩. Accessed 19th March 2022.
Mannini, P., Genovesi, R., Letterio, T., 2013. IRRINET: large scale DSS application for on-farm irrigation scheduling. Procedia Environ. Sci. 19 (0), 823–829.
Martin-Candilejo, A., Santillán, D., Garrote, L., 2020. Pump efficiency analysis for proper energy assessment in optimization of water supply systems. Water 12 (1), 132.
Melton, F.S., Huntington, J., Grimm, R., Herring, J., Hall, M., Rollison, D.,. & Anderson, R.G. (2021). OpenET: Filling a critical data gap in water management for the western united states. JAWRA Journal of the American Water Resources Association.
Melton, F.S., Johnson, L.F., Lund, C.P., Pierce, L.L., Michaelis, A.R., Hiatt, S.H., Guzman, A., Adhikari, D.D., Purdy, A.J., Rosevelt, C., Votava, P., 2012. Satellite irrigation management support with the terrestrial observation and prediction system: a framework for integration of satellite and surface observations to support improvements in agricultural water resource management. IEEE J. Sel. Top. Appl. Earth Obs. Remote Sens. 5 (6), 1709–1721.
Moorhead, J.E., Marek, G.W., Gowda, P.H., Lin, X., Colaizzi, P.D., Evett, S.R., Kutikoff, S., 2019. Evaluation of evapotranspiration from Eddy covariance using large weighing lysimeters. Agronomy 9 (2), 99.
Morel, J., Kumar, U., Ahmed, M., Bergkvist, G., Lana, M., Halling, M., Parsons, D., 2021. Quantification of the impact of temperature, CO_2, and rainfall changes on swedish annual crops production using the APSIM model. Front. Sustain. Food Syst. 5, 178.
Myrbeck, Å., 1998. Swedish agricultural and horticultural crops. PM-Kemikalieinspektionen-KEMI, Sweden.
Novelli, F., Spiegel, H., Sandén, T., Vuolo, F., 2019. Assimilation of sentinel-2 leaf area index data into a physically-based crop growth model for yield estimation. Agronomy 9 (5), 255.
Pereira, L.S., Paredes, P., Melton, F., Johnson, L., Mota, M., Wang, T., 2021. Prediction of crop coefficients from fraction of ground cover and height: practical application to vegetable, field and fruit crops with focus on parameterization. Agric. Water Manag. 252, 106663.
Pereira, L.S., Paredes, P., Melton, F., Johnson, L., Wang, T., López-Urrea, R., Cancela, J. J., Allen, R.G., 2020. Prediction of crop coefficients from fraction of ground cover and height. Backgr. Valid. Using Ground Remote Sens. data. Agric. Water Manag. 241, 106197.
Phocaides, A., 2000. Technical handbook on pressurized irrigation techniques. FAO, Rome, p. 372.
OpenET. (2021). Available at: ⟨https://openetdata.org/⟩. Accessed 31st January 2021.
Renew Economy. Available at: ⟨https://reneweconomy.com.au/nuclear-power-takes-a-hit-as-european-heatwave-rolls-on-87477/⟩. Accessed 24th May 2020.
Riksbanken (2018). Avialble at: ⟨https://www.riksbank.se/globalassets/media/rapporter/ppr/fordjupningar/engelska/2018/small-effects-on-production-and-inflation-of-the-summers-drought-and-forest-fires-article-in-monetary-policy-report-september-2018.pdf⟩. Accessed: 31st January 2021.
Scott Lee Davis (2020). Google Earth Toolbox (⟨https://www.mathworks.com/matlabcentral/fileexchange/12954-google-earth-toolbox⟩), MATLAB Central File Exchange. Retrieved August 6, 2020.
Shannak, S., Mabrey, D., Vittorio, M., 2018. Moving from theory to practice in the water–energy–food nexus: an evaluation of existing models and frameworks. Water-Energy Nexus 1 (1), 17–25.
SMHI, Analysmodell MESAN. (2020b). Available at: ⟨https://www.smhi.se/data/oppna-data/meteorologiska-data/analysmodell-mesan-1.30445⟩. Accessed 23rd August 2020.
SMHI. (2020a). Available at: ⟨https://www.smhi.se/klimat/klimatet-da-och-nu/manadens-vader-och-vatten-sverige/manadens-vader-i-sverige/juli-2018-langvarig-hetta-och-svara-skogsbrander-1.137248⟩. Accessed 11th April 2021.
SPEI Global Drought Monitor, Available at: ⟨https://spei.csic.es/map/maps.html#months=0#month=11#year=1958⟩. Accessed 24th May 2020.
Statistics Sweden. (2018) Standard yields for yield survey districts, counties and the whole country in 2018. Available at: ⟨https://www.scb.se/publication/35137⟩. Accessed 31st January 2021.
Statistics Sweden. (2021). Available at: ⟨http://www.statistikdatabasen.scb.se/pxweb/en/ssd/START_MI_MI0902_MI0902E/VattenAnvJord/⟩. Accessed: 31st January 2021.
Statistics Sweden. (2022a). Available at: ⟨https://www.scb.se/en/finding-statistics/statistics-by-subject-area/agriculture-forestry-and-fishery/agricultural-production/production-of-potatoes/pong/statistical-news/production-of-potatoes-in-2018.-preliminary-data/⟩. Accessed: 14th March 2022.
Statistics Sweden. (2022b). Available at: ⟨https://www.scb.se/hitta-statistik/statistik-efter-amne/jord-och-skogsbruk-fiske/jordbrukets-produktion/skord-av-potatis/⟩. Accessed: 14th March 2022.
STRÅNG. Available at: ⟨http://strang.smhi.se/⟩. Accessed 23rd August 2020.
SWEDIMS. Available at: ⟨www.swedims.se⟩. Accessed 9th April 2022.
Swedish Board of Agriculture. (2007). Bevattning och växtnäringsutnyttjande. Available at: ⟨https://webbutiken.jordbruksverket.se/sv/artiklar/bevattning-och-vaxtnaringsutnyttjande.html⟩. Accessed 17th October 2020 (in Swedish).
Swedish Board of Agriculture. Available at: ⟨https://jordbruksverket.se/e-tjanster-databaser-och-appar/e-tjanster-och-databaser-stod/kartor-och-gis⟩. Accessed 24th May 2020.
The Local. Available at: ⟨www.thelocal.se/tag/drought⟩. Accessed 24th May 2020.
USDA NRCS. (1997). Irrigation guide. National Engineering Handbook, 452. Available at: ⟨http://www.nrcs.usda.gov/Internet/FSE_DOCUMENTS/nrcs141p2_017641.pdf⟩.
USDA. (2022). National Agricultural Statistics Service. Available at: ⟨https://quickstats.nass.usda.gov/⟩. Accessed 19th March 2022.
Stepanovic, S., Rudnick, D., Kruger, G., 2021. Impact of maize hybrid selection on water productivity under deficit irrigation in semiarid western Nebraska. Agricultural Water Management 244, 106610.
Wagner, M.P., Slawig, T., Taravat, A., Oppelt, N., 2020. Remote sensing data assimilation in dynamic crop models using particle swarm optimization. ISPRS Int. J. Geo-Inf. 9 (2), 105.
Wang, W., Cui, Y., Luo, Y., Li, Z., Tan, J., 2019. Web-based decision support system for canal irrigation management. Comput. Electron. Agric. 161, 312–321.
Weslien, P. (2020, June 1). Personal interview.
Williams, J.R., Jones, C.A., Kiniry, J.R., Spanel, D.A., 1989. The EPIC crop growth model. Trans. ASAE 32, 497–511.
Zhang, C., Zhang, M., Sun, X., 2012. Henan zhaokou irrigation management system design based on flex viewer. Procedia Eng. 28, 723–728.
Zhang, J., Campana, P.E., Yao, T., Zhang, Y., Lundblad, A., Melton, F., Yan, J., 2018. The water-food-energy nexus optimization approach to combat agricultural drought: a case study in the United States. Appl. Energy 227, 449–464.
Zhang, Y., Song, C., Sun, G., Band, L.E., McNulty, S., Noormets, A., Zhang, Z., 2016. Development of a coupled carbon and water model for estimating global gross primary productivity and evapotranspiration based on eddy flux and remote sensing data. Agric. For. Meteorol. 223, 116–131.
Zhou, Z., Andersen, M.N., Plauborg, F., 2016. Radiation interception and radiation use efficiency of potato affected by different N fertigation and irrigation regimes. Eur. J. Agron. 81, 129–137.
Zhou, Z., Plauborg, F., Parsons, D., Andersen, M.N., 2018. Potato canopy growth, yield and soil water dynamics under different irrigation systems. Agric. Water Manag. 202, 9–18.
Zotarelli, L., Dukes, M.D., Romero, C.C., Migliaccio, K.W., Morgan, K.T., 2010. Step by step calculation of the Penman-Monteith Evapotranspiration (FAO-56 Method). Institute of Food and Agricultural Sciences. University of Florida.